KWAME NKRUMAH UNIVERSITY OF SCIENCE AND TECHNOLOGY

COLLEGE OF ENGINEERING

DEPARTMENT OF GEOMATIC ENGINEERING

SPATIAL MAPPING OF CARBON STOCK IN MANGROVES IN THE ELLEMBELLE DISTRICT, GHANA.

A THESIS SUBMITTED TO THE DEPARTMENT OF GEOMATIC ENGINEERING, KWAME NKRUMAH UNIVERSITY OF SCIENCE AND TECHNOLOGY IN PARTIAL FULFILMENT OF THE REQUIREMENTS FOR THE DEGREE OF

MASTER OF PHILOSOPHY IN GEOMATIC ENGINEERING

BY

LILY LISA YEVUGAH

SUPERVISORS

DR E. M. OSEI JNR

REV. JOHN AYER

October, 2016

DECLARATION

I hereby declare that this thesis is my own work and does not contains materials previously published by any other person nor material which has been accepted for the award of any other degree of any university, except where due acknowledgment has been made in the text.

Yevugah, Lily Lisa …… ……..…..

Student Name Signature Date

Certified by:

Dr. Edward M. Osei Jnr. …… ……..

Supervisor Signature Date

Certified by:

Rev. John Ayer …… ……..

Supervisor Signature Date

Certified by:

Dr. Isaac Dadzie …… ……..

Head of Department Signature Date

DISCLAIMER

This document describes work undertaken as part of a programme of study at the Kwame Nkrumah University of Science and Technology (KNUST), Kumasi, Department of Geomatic Engineering. All views and opinions expressed therein remain the sole responsibility of the author, and do not necessarily represent those of the institute.

DEDICATION

I dedicate this thesis to my family for the affection, love, encouragement and the daily prayers that has seen me through.

A special feeling of gratitude to my loving parents Sylvanus and Fidelia Yevugah whose words of encouragement and push for tenacity ring in my ears. To my sisters Vera and Louisa and my brothers Anthony, Perron and Cherry for their love and constant support.

I will always appreciate what they have done for me.

ACKNOWLEDGEMENT

Sincere thanks and appreciation goes to the Almighty God for good health and wellbeing that were necessary to complete this research. I wish to express my sincere thanks to my supervisors Dr. E. M. Osei Jnr. and Rev. John Ayer for their valuable guidance and encouragement necessary for this research.

I am very grateful to Joshua Osei Nti, Beatrice Acheampong and Richard Ansah for their constant help and support throughout this research. I also express my gratitude to the Head of Department Prof. Ing. Collins Fosu and the entire staff of the department of Geomatic Engineering.

I express my gratitude to Mr. Emmanuel Donkor, Mr. Benjamin Torgbor and the entire staff of Forestry Commission in Kumasi, Accra and Tarkwa.

I thank my family and friends for the unceasing encouragement, support and attention.

ABSTRACT

Compared to other wetland ecosystems, mangroves are well known for their numerous ecosystem services, especially carbon pool. In Ghana, however, there is limited information on the sequestered carbon in mangroves. There is increasing interest on national climate change mitigation and adaptation plans in mangroves in developing nations, and Ellembelle in the Western Region of Ghana is of no exception. Ellembelle, the study area, is one of the areas where the little information on the size and variation of mangrove carbon stock needs to be addressed. This research, therefore, aimed at determining the carbon stock from the carbon sequestered in mangrove and the areal extent in mangrove forest. It also aimed at determining the changes that has occurred over the years 1991, 2000 and 2015, and the prediction for 2025. The spatial map of the mangrove forest was obtained using a random forest classification algorithm to determine the Land Use and Land Cover (LULC) for the mangrove forest in Ellembelle in the Western Region of Ghana. The accuracy assessment for the classified images of 1991, 2000 and 2015 are 76.16%, 82.45% and 81.13% respectively; with kappa of 0.70, 0.78 and 0.76 respectively. The mangrove cover in 1991 was 298.35 ha, in 2000 it increased to

350.01ha and further increased in 2015 to 374.49ha. A change map was used to determine the changes of mangrove in the years 1991 to 2000 and 2000 to 2015. A Markov chain analysis used to predict mangrove extent showed that mangrove will increase to 381.69ha in 2025. The ecosystem carbon density estimate for the mangrove forest was weighted based on their spatial distribution across the landscape to yield a total carbon stock of for the Ellembelle mangrove forest. The error obtained from the 95% Confidence Interval was ± 1.53%, which is within the acceptable levels of uncertainty based on the Monte Carlo Analysis. The overall carbon estimated for 2015 based on the area for mangrove was 1,550,295 tons with an uncertainty of ±57,125.40 tons.

TABLE OF CONTENT

LIST OF TABLES

LIST OF FIGURES

LIST OF ABBREVIATIONS

AGB	**Above Ground Biomass**
AGC	**Above Ground Carbon**
AOI	**Area of Interest**
BGB	**Below Ground Biomass**
BGC	**Below Ground Carbon**
CA	**Cellular Automata**
CDM	**Clean Development Mechanism**
CI	**Confidence Interval**
CO2	**Carbon Dioxide**
CREMA	**Community Resource Management Area**
DBH	**Diameter at Breast Height**
ETM	**Enhanced Thematic Mapper**
FAO	**Food and Agriculture Organization**
FD	**Forestry Department**
GHG	**Green House Gasses**
GIS	**Geographic Information Systems**
LULC	**Land Use Land Cover**
LULCC	**Land Use Land Cover Change**
ML	**Maximum Likelihood**
NIR	**Near Infrared**
OA	**Overall Accuracy**
PSP	**Permanent Sample Plot**
REDD	**Reducing Emission from Deforestation and Forest Degradation and Enhancing Forest Carbon**
RF	**Random Forest**
RMSE	**Root Mean Square Error**
RS	**Remote Sensing**
SE	**Standard Error**
TOA	**Top of the Atmosphere**

TCS	**Total Carbon Stand**	**TM Thematic Mapper**

CHAPTER 1

INTRODUCTION

1.1 Background Information

Mangroves forests are traditionally considered as one of the world's most productive ecosystem (Kathiresan and Qasim, 2005). Mangrove ecosystem provides surrounding habitats with many ecological services and can be exploited to the benefit of mangrove communities. Irrespective of their numerous benefits, they are however under threat from lots of human activities which is causing large mangrove forest areas to be lost. It is therefore necessary to know the state of the mangrove forest and the area it covers in order to know the extent of deforestation of mangroves.

Mangrove trees have unique adaptations to the severe conditions of coastal environments. Research shows that mangrove forests are rated as one of the carbon richest forests. According to Donato *et al*. (2011), mangrove forests in the tropics contains an average of 1,023 tons carbon per ha. Deforestation gives out about 0.02 – 0.12 Pg carbon per year, while storing up to 20 Pg C every year. Mangrove forests are practically highest sequesters of carbon and their ability to sequester carbon reduces as they reach maturity (Mukherjee, 2007). Salt marshes globally absorbs lots of carbon. Mangroves swamp with its wealth in stored carbon provides a potential sink for atmospheric carbon. However if mangroves are not well catered for they may become the sources of Green House Gases (GHG) in the likes of carbon and methane. Compared to other forest wetland ecosystems, salt marshes, mangroves and sea grass beds can store large amounts of carbon. This is possible for two main reasons: (1) Plants usually grow a lot each year, and for that reason a large amount of Carbon Dioxide (CO_2) is sequestered; and (2) the soils are without oxygen so carbon that gets incorporated into the soils decomposes quite slowly and can persist for hundreds or even thousands of years (NOAA, 2016). Aside the ability to sequester large amount of carbon, mangrove forest is a habitat for very large variety of fish,

crab, shrimp and mollusc species. These fisheries serve as source of food for thousands of coastal communities and the mangrove forest also serves as a nursery for many fish species including coral reef fish. Wood obtained from mangroves are unaffected by decay and pests, making it extremely valued. Most of the local communities also depend on mangroves for building material and firewood. Some use the mangrove plant as medicine and the leaves as animal fodder. In recent times, there are reports on commercially harvesting for pulp, wood chip for charcoal production.

Appropriate and cost effective methods are required to reduce the laborious method of manually calculating for the amount of carbon sequestered. Remote Sensing (RS) is noted for giving a good classification of mangroves. Therefore, integrating RS and Geographic Information Systems (GIS) will be an option in this regard. Seller *et al*. (1995) and Bastiannssen *et al*. (1998) have used RS for the estimation in plant biomass. RS approach can be used for carbon sequestration by establishing permanent sample plots by making use of fixed coordinates (MacDicken, 1997). Tucker (1979), Richardson *et al*. (1983) and Christensen and Goudriaan (1993) have shown that Near Infra-Red (NIR) radiation contains significant details about plant biomass. Remotely sensed satellite data can therefore be used to compute the biomass and eventually carbon sequestration value of mangrove in a larger area to save time and money (Tripathi *et al*., 2010).

Mangrove forests trap sediments flowing down rivers and off the land by virtue of their dense root system and this helps stabilize the coastline and prevents erosion. This research is based on the integration of RS and GIS in estimating the spatial extent of mangrove and the rate of change of mangrove in the Ellembelle district in Ghana. It also determine how much carbon is stored in mangrove thereby giving an estimate of how much carbon is sequestered in mangroves in the study area.

1.2 Research Motivation

The research is conducted along the Amanzule River at Ellembelle district. The area is covered with mangrove. Although the indigenes benefits greatly from the mangrove forest, mangrove forests are vulnerable to both residents and outsiders. The study area falls outside the 5 selected wetlands under the Ramsar Convention of 1975. The mangroves found in this area are generally managed by the indigenes of the place based on their local community rules. The amount of carbon that is sequestered in mangrove at Ellembelle district has not been determined. Thus, the research gives an idea of the areal cover of mangrove and the rate of change in mangrove at Ellembelle District in Ghana. It predicts how much change will occur in the next decade of 2025. Allometric equations are employed in this research to determine how much carbon is stored in mangrove thereby giving a good estimation of how much carbon is sequestered in mangroves in Ellembelle.

1.3 Prior Work

Several research work have been carried out in this field of research. In Ghana, Ajonina (2011) researched on the rapid assessment of mangrove status for payment for ecosystem services in Amanzule in the Western Region for ecosystem services. His research was along the stretch of the mangrove sites in western region. He did a quick assessment on the carbon sequestered in mangrove along the stretch of the western region of which some sample plots in Amanzule were chosen. Mensah (2013) used RS technology to map out previous and current areal extent of mangrove in the Ellembelle District in the Western Region. In this research, Landsat Thematic Mapper and Rapideye imagery where used to determine the land use and land cover map of the area. The Forestry Department (FD) of the Food and Agriculture Organization (FAO) of the United Nation did a global forest resource valuation on the thematic study on mangrove in Ghana. A similar work with the use of Remote Sensing (RS) was done by Viaphasa (2006) whose research work was on the use of RS techniques for mangrove mapping.

The main objective for the research was to unveil the potential of some of the unexplored remote sensing techniques for mangrove studies focusing on improving the separating ability of classes between mangrove species or community types. Chen *et al*. (2013), researched on the multi decadal mangrove forest change detection and prediction in Honduras, Central America, with Landsat Imagery and a Markov Chain Model. They investigated the spatiotemporal changes in Honduras and the future trend of mangrove.

1.4 Problem Statement

Carbon emission is a cause for global warming. This is a feared problem all over the world. Mangroves are good carbon sinks but there are uncertainties in their carbon stock since much is not known about their areal extent (Bouillon *et al*., 2008). This can be noted in the Ellembelle district where the amount of carbon that is sequestered in mangrove has not been determined. Over the past century, burning, deforestation and urbanization activities have contributed to increased level of CO_2 and other GHG in the atmosphere (Waran, 2001). CO_2 is a common contributor of GHG causing global warming. This results in an increase in sea level. Mangroves, however, are known to be good carbon sequesters. Mangroves absorbs more carbon than they emit. Knowing the amount of carbon sequestered is usually done by measuring directly on the field, the biomass of dried plant species. There are many conventional method that are used for quantification of stored carbon. Most of these methods are labour and cost intensive in terms of the coverage. These limitation hinders comprehensive calculation and monitoring of carbon.

Bouillon *et al*. (2008), explains that mangroves serves as good carbon sink but there are uncertainties in the carbon stock since much is not known about their areal extent. Also, appropriate and cost effective methods are required to reduce the laborious method of manually calculating for the amount of carbon sequestered. There should be a good but cost effective

means of determining the amount of carbon sequestered. Since RS is noted for giving a good classification of mangroves, integrating it with GIS offers an option in estimating the amount of carbon sequestered (Seller *et al*., 1995; Bastiannssen *et al*., 1998; MacDicken, 1997; Tucker (1979), Richardson *et al*., 1983; Christensen and Goudriaan, 1993; Tripathi *et al*., 2010).

1.5 Aims and Objectives

The research aims at mapping out mangrove forest from 1991 to 2015. It further aims at determining the amount of carbon sequestered in mangrove using allometric equations and RS. The objectives of the research are to:

1. map mangrove forest using RS and GIS.
2. assess of mangrove forest change using RS.
3. predict the loss and gain of mangrove by 2025.
4. determine the amount of sequestered carbon within the study area.

1.6 Research Questions

Based on the above research objectives, the following research question were formulated to help achieve the objective for these research:

1. What is the extent of Mangrove forest?
2. What are the changes in the extent of mangrove forest over the period of 1991 to 2000 and 2000 to 2015?
3. What will be the extent of mangrove forest in 2025?
4. How much carbon is sequestered in the Mangrove forest?

1.7 Research Approach

The research approach adopted is enumerated as follows:

- RS techniques is used to answer questions one that is extent of Mangrove forest. In this case, classification is employed to determine the land use land cover (LULC) map. The classification is based on the Random Forest (RF) algorithm.
- To map change and extent of mangrove forest over the period of 1991 to 2015, a GIS analysis method based on change matrix was employed to determine the areal change of the LULC between the years 1991 to 2000 and 2000 to 2015. This approach was used to answer question two.
- To answer the third research question, the application of the Markov chain analysis and the Cellular Automata (CA) Markov was used to project and model changes of the LULC for the year 2025.
- Determination of the sequestered carbon in mangrove which answers the fourth research question was done through field measurement of mangrove trees and application of allometric equation to determine the Above Ground Biomass (AGB) and the Below Ground Biomass (BGB) which aided in the determination of the carbon.

1.8 Thesis Structure

The content of the research is structured under the following chapters:

Chapter one gives an introduction to the research work. It highlights on prior research work based on mangrove and sequestered carbon. The main aim and the general objectives of the research is highlighted within this chapter. This chapter also show the problem statement and the research motivation.

Chapter two gives a theoretical and conceptual discourse of mangrove and carbon sequestration in mangrove. Literature review on mangroves and further talks about climate change, effect of climate change, GHG, carbon sequestration and sequestered carbon mangrove pertaining to the

research are highlighted. This chapter further researches on the various RS methods that have been employed in similar study and the use of Markov Chain analysis.

The methods and processes involved in the mapping of areal extent of mangrove and the determination of sequestered carbon as well as the forecasting are explained in chapter three. Chapter four shows the results obtained from the research. Analysis and discussions are carried out on the result.

The conclusions and recommendations drawn from the research are presented in chapter five.

CHAPTER 2 SPATIO-TEMPORAL ANALYSIS OF MANGROVE

2.1 Mangroves

Mangrove trees are indigenous species and a major contributor to marine environment. Mangrove is a halophyte; a plant that thrives in salty condition. It has the ability to grow where no other tree can. As defined by Mitch and Gosselink (2007), mangroves are association of halophytic tree, shrubs and other plant growing in brackish to saline tidal waters found along the tropical and subtropical sheltered coastline. Mangrove forests provides wood and non-wood forest products, coastal protection, and conservation of biological diversity and also provides habitat, breeding grounds and nutrients for a variety of fish and shellfish. Mangrove swamps serves as a link to freshwater and hosts a rich diversity of animal species. There are about 68 mangrove obligate species found globally (Gisen *et al*., 2007). Mangrove species are found within these two Northern and Southern hemisphere and are vastly different in both size and structure (Tomlinson, 1999).

The structure and functions of mangroves diverges significantly depending on the topography, substrate, latitude and hydrology (Saenger and Snedaker, 1993). Mangroves are classified into four major associations of different structure in relationship with features and the environment in which they exist (Cintron *et al*., 1978; Mitch and Gosselink, 2007). They are:

- Fringe/Coastal mangroves;
- Riverine /Estuarine mangroves;
- Basin mangroves; and
- Dwarf scrub mangroves.

Mangrove species have unique adaptations for survival. Noteworthy amongst this survival includes gas exchange through the stilt roots and pneumatophores. Some species re-sprout whiles others fill vacant growing spaces in response to canopy disturbances (Kauffman & Cole, 2010).

2.2 Mangroves in Ghana

In Ghana, Mangroves are mostly limited to stands about the lagoons and some estuaries. According to the UNEP (2007), mangrove forests cover about 137 km^2, making up approximately 0.2% of the 1,342 km^2 of entire forest area in Ghana (Gordon and Ayivor, (2003); UNEP, (2007); Spalding *et al*., (2010). Mangroves in Ghana are mostly found at Apam Muni Lagoon, Winneba, Sakumono 1 Lagoon, Botwiano, Korle Lagoon, Teshie Sakumono 2 lagoon, Ada, Sroegbe and Keta Lagoon (Diop, 1993)

There are various species of mangrove in Ghana according to UNEP (2007). *Avicennia germinans, Conarcarpus erectus, Laguncularia racemosa* and *Acrostichum aureum* are found around the lagoon Ajonina (2011). The mangrove swamp are restricted in area and distribution, and rarely developed beyond a thicket stage; *Laguncularia racemosa* and *Rhizophora racemosa, Rhizophora mangle* are found on the seaward side of lagoons in saline conditions. *Avicennia germaninanson* the inland side of the swamps (FAO, 2005).

In Ghana mangrove are renowned for creating home for most animal species. Mangrove afforestation falls under a Clean Development Mechanism (CDM) project. Comparatively to other land forests, mangrove ecosystem collects sequestered carbon in the sediments (Wojick, 1999). According to Heumann (2011) and Kuenzer *et al*. (2011), the value of mangroves is widely recognized in this present years. Ramsar Convention on Wetlands and Kyoto Protocol highlights on the significance of protection and conservation activities to mitigate loss of mangroves.

2.3 Importance of Mangrove

Mangroves play vital ecological roles as well as economic roles, particularly in the neighbouring communities. The commercial value for mangrove is rated at $600,000 for each year according to Mensah (2013).

Mangrove forests serves as the home to a very large variety of fish, crab, shrimp and mollusc species. Crabs are usually found in mangroves area because they feed on the fallen leaves in mangroves. These fisheries serves as source of food for many of coastal communities aside that the mangrove forest also serves as a nursery for many fish species that includes coral reef fish.

Mangrove wood is resistant to decay and insects infestations making it very valuable. Most communities rely on this wood for construction material as well as for wood fuel. These communities also collect medicinal plants from mangrove ecosystems and use mangrove leaves as animal fodder. Mangrove trees are reported to be harvested for pulp, and charcoal production. Mangrove roots trap deposits that flows down the rivers and off the land. This prevents erosion from waves and storms.

2.4 Threats to Mangroves

High population pressure along the coast has led to the conversion of mangrove areas to other uses leading to mangrove losses over time. Mangrove forest serves as key to good coastal ecosystems but irrespective of this fact, there has been an alarming speed in the disappearance of the Mangrove forest. Thailand has lost 84% of its mangroves. This is recorded as the highest mangrove lost in any nation (Berlanga-Robles, 2011). Mangroves are known to be resilient to natural disturbances. Mangrove ecosystems worldwide are highly endangered by human activities. Threats to mangrove forest are usually perpetrated by the LULCC as well as the global climatic change. Mangrove forests are often seen to be unproductive and smelly for this reason they are deforested to create agricultural land, human settlement and infrastructure such as harbours and industrial area. Some also clear them to make room for tourist developments, shrimp aquaculture and salt farms. These reasons are major factors from which mangroves are

being lost. According to Valiela *et al*. (2001) and Giesen *et al*. (2007), land conversion has given rise to loss greater than 35% of mangrove since 1980 to 2000.

Mangrove trees are known to serve as good firewood and construction wood, wood chip and pulp, charcoal production and animal fodder. For these uses mangrove are subjected to over harvesting. Harvesting of mangroves has been ongoing in some places for centuries now it has reached a level where it is no more sustainable; thus threatening the future of mangrove forests. The use of fertilizers, pesticides and some toxic artificial chemicals carried by river systems from sources upstream can destroy animals in mangrove forests while oil pollution can smother mangrove roots and suffocate the trees. If salinity of the river or lagoon is too high, the mangroves cannot survive (Kathiresan and Rajendran, 2005). Inflow of freshwater can cause mangroves to dry out. Erosion as a result of land deforestation can massively cause increase in the amount of sediment in rivers. This can overcome the mangrove forest's filtering ability, leading to the forest being clogged.

Mangrove forests are being lost due to all its benefits with a lesser recognition being given to the effect of the loss of the mangrove forest. Ghana's mangrove is said to have decreased considerably in the past decades (Adjonina, 2011). The loss of mangrove is a continual thing because of the continual growth of population and lack of mitigation effect established to control the loss of mangrove.

In spite of the importance of mangrove ecosystem being effective carbon sinks, much has not been done in view of the uncertainties in their carbon stock estimates because of the uncertainties in their areal extent. Because of the threats posed on the mangroves ecosystem, structures and ecosystem carbon pool are being monitored. Based on this, programs set for carbon mitigation Reducing Emission from Deforestation and Forest Degradation and

Enhancing Forest Carbon Stocks in Developing Countries (REDD+) and other sorts of financial incentives have been associated to the conservation of the mangrove forest.

2.5 Mangrove and Climate Change

Mangroves are appropriate for climate change mitigation, because they are known to be one of the best carbon sequesters. Mangrove forest ecosystem have received a greater recognition for the past few years because of their ability to sequester GHG. Recent climate change mitigation efforts have focused on the reduction of GHG particularly CO_2 through the conservation and restoration of natural systems recognized as effective carbon sinks (Trumper *et al*., 2009). REDD+ mechanism helps reduce global GHG and makes amends for conservation and sustainability and the enhancement of forest (Nellerman *et al*., 2009; Duarte *et al*., 2005).

Mangrove forest soils can sequester six times the carbon CO_2 of tropical rainforests per hectare in a year (Donato *et al*., 2011). Preserving the Mangrove forest may not only prevent extra release of Carbon but contributes in sequestering more carbon than other forest types.

2.6 Estimation of Mangrove Biomass

Forest naturally serves as a storage for large quantities of carbon. These storage adds up to the carbon dioxide in the atmosphere when they are cleared. The mass of living organisms in a forest is termed biomass. To estimate this it requires that one captures all living organism within the area and weigh its mass on a scale. In calculating biomass of an area, the animals and herbaceous plants form part of the biomass but their contribution serves as a very minute composition hence they are usually ignored. The biomass in a forest is most often considered as trees.

Within the context of ecosystem biomass, mangroves can be categorized into five carbon pools:
1) AGB of live mangrove;

2) BGB of live vegetation;

3) Dead wood;

4) Litter and 5) Soil.

Together the AGB and the BGB make up the living biomass. Litter refers to the leaves that have dropped in the forest whiles the ground dead wood, comprises of the down dead. The quantification of biomass is important as an indicator of carbon stored in forests. If BGB is not included in the accounting of deforestation, emissions to the atmosphere would be underreported, in afforestation or reforestation, sequestration rates would be underreported (Githagia, 2013).

There are three main methods used in estimating forest biomass, these are; the harvest method, the tree method and the allometric method. According to Komiyama *et al*. (2005), the total weight of any individual tree within a mangrove forest often reaches several tons. This means that the harvest method cannot be used for matured forests which in itself is not reproducible because all the trees may be destructively harvested. The mean tree method is utilized only in forest with a homogeneous tree size distribution, such as a plantation. The allometric method estimates the whole or partial weight of a tree from measurable tree dimensions, including trunk diameter and height using allometric equation. The use of the allometric equation is termed as the non-destructive method of estimation and hence useful for estimating temporal changes in forest biomass.

2.7 Allometric Equation

Allometric equations for mangroves have been developed for several decades to calculate biomass and subsequent growth. Most studies have used allometric equations for single – stemmed tree forms, as mostly seen *in Rhizophora, Avicennia* and *Excoecaria*species (Clough *et al*., 1997). Clough *et al*., (1997) showed that the allometric relationship can be used for trunks in a multi stemmed tree. Moreover, allometric relationships have been used to estimate the

biomass of dwarf mangrove trees. Clough *et al*. (1997) found different relationships in different sites, although Ong *et al*. (2004) reported similar equations applied to two dissimilar sites for *Rhizophora apiculata*. This issue is important for practical uses of allometric equations because if the equations are segregated by species and site then different expression can be established for each site.

Different equations can yield very large differences when predicting biomass Chave *et al*. (2005), Komiyana *et al*. (2005). The differences in estimates of biomass of trees with larger Diameter at Breast Height (DBH) can be dramatic. The measurement of DBH is more practical than other parameters as close canopies tree heights are not easy to measure. In this research the allometric equations used, were developed by the Forestry Commision of Ghana and they were based on several equations including those of Komiyana *et al*. and Chave *et al*. However the densities of the various mangrove species are based on the weighted mangrove species found in Ghana

2.8 Quantifying Uncertainty in Carbon Pool

Estimation of carbon stock is based on sampling a population of interest for example one forest stratum, rather than taking measurements of the entire population. The purpose of sampling is to achieve a representative data set of the population in as efficient a manner as possible. (Goslee *et al*., 2010). For carbon assessment, it is essential that uncertainty is reported for carbon pool. Uncertainty reflects the degree of precision in the dataset (Kauffman and Donato, 2012). Carbon assessment is typically reported as 95% Confidence Interval (CI) which is expressed as a percentage of the mean. Uncertainty in component pools is determined by 95%CI Half-width which is expressed as the mean $\pm$2 times the standard error (SE) of the mean. Mathematically Uncertainty therefore is expressed as 100*(95%CI half width)/mean.

In calculating the total carbon, Pearson *et al*. (2005, 2007), GOFC-GOLD (2011), describe two methods for computing the total uncertainty for carbon stock. The initial method uses "simple error propagation" that is achieved by finding the Root Mean Square (RMS) of the sum of the squares of the component errors. The second method uses the Monte Carlo simulation to propagate error. The first method is simple and easy to use, however the second method requires an additional computer software. Monte Carlo is used when substantial correlation exists between datasets and when the uncertainties are very large. In theory however, Monte Carlo analysis is deemed robust to any data structure. Kaufmann and Donato (2012) however highlights that the difference in results obtained through the simple error propagation and the Monte Carlo analysis are typically small unless correlations or uncertainties are very high (Pearson *et al*., 2007).

2.9 Remote Sensing of Mangrove Forest

Mangrove forest are usually swampy and marshy areas, because of the daily inundation of water which makes it very difficult monitoring the ecosystem from field data alone. RS is widely used to measure biomass in wetlands. The remotely sensed data and the methods used for characterizing mangrove ecosystems have advanced over time, upgrading from a traditional RS approach to a more advanced one. Traditional approach includes the use of Aerial Photograph (AP) and some high resolution systems (Heumann, 2011; Green *et al*., 1998). In the case of AP, visual inspection was carried out. Over the years, RS applications involves the use of high and low resolution satellite imagery like Landsat, SPOT and ASTER. Some of the methods used to detect mangrove have involved supervised and unsupervised classification or a combination of both.

Over the years RS has played a major role in mapping and understanding changes in the areal extent and the spatial pattern of mangrove forest related to natural disasters and anthropogenic

forces. Vaiphasa *et al*. (2006) and Heumann (2011), said that the progression in RS techniques promises in-depth and more accurate mangrove mapping.

According to Fatoyinbo and Simard (2013), two distinct methodologies are used for estimating mangrove biomass from RS data:

- By using passive optical data and average biomass values and
- Through height or volume measurement.

Passive RS makes use of visible and NIR reflectance to form images. This RS data is the basis satellite mapping prior to the increasing sensors such as Landsat, MODIS, etc., that gives greater ease of image interpretation. Optical measurements have been extensively used in studies that creates a connection between AGB measurements obtained from field to satellite observations. The problem associated with the optical data is the presence of cloud cover, especially in the tropics and this creates difficulties in the usage of the data. The simplest way to estimate biomass is to determine the land cover and then assign a value to each land cover type. With biomass it is easier to estimate AGB through this means as much consideration is not given to the differences in structure. However the error associated with this is great especially with a larger area of heterogeneous forest (Goetz *et al*., 2009).

2.9.1 Classification algorithms

A number of algorithms have been developed in recent years for machine learning for RS applications. These algorithms are the support vector machines, the neural networks and the RF. In the methods of RS application especially with classification, the general methods have been to determine models that will statistically determine radiance value recorded by sensors through grouping them into classes or categories. However, according to Elith *et al*. (2008), these methods are based on the precept that the data model is used and the parameters is estimated from it. A typical example of the use of this traditional method is the Maximum

Likelihood (ML) classifier model. The assumption is that image data for each category together with the training data are of a normal distribution.

A machine learning approach on the other hand studies the relationship between the predictors and response data (Brieman, 2001). This technique is being used quite recently for image classification and creation of continuous variable such as the forest biomass of a given area. There is an increasing use of this algorithm in the area of satellite and image classification (Horning, 2010).

RF uses results obtained from different models to determine a response. This is termed as the ensemble model. Using RF, numerous decision trees are generated and the response is calculated based on the outcome of all the decision trees. Decision tree are predictive models used in setting binary rules to calculate target values. Decision trees are made up of two types, the Classification and Regression trees used to create continuous data sets such as biomass and percent tree cover. RF like decision trees can be used to solve classification and regression problems and this can overcome drawbacks that comes with single decision trees while preserving the benefits. In the case of classification, Breiman and Cutler (2004), states that the most predicted class assigned to an object in the case of regression, the resultant value for that object is average of the predictions. Predictions from RF are derived using a forest of trees.

RF has numerous benefits as compared with different methods of image classification. It is non-parametric, uses continuous and categorical data sets, easy to parameterize, not sensitive to over-fitting, better at dealing with outliers in a data set, and it calculates ancillary information; classification error and variable importance (Horning, 2010).

2.9.2 Classification using Random Forest

Jhnonrie *et al*. (2015) researched on how to assess the accuracy of RF classification rule using object based image analysis (OBIA) application (eCognition Developer) and the results were compared with common pixel-based classification algorithm ML for mangrove land cover mapping in Kembung River, Bengkalis Island, Indonesia. Overall accuracy (OA) as well as user and producer accuracies and Kappa statistic were used to compare classification results. The results showed that the more data model used produced higher OA and kappa statistics for RF classifier as compared to ML. The best mangrove discrimination is found using RF classifier. This was achieved by combining Landsat 5 TM with SAR, together with spectral transformations. The ML classifier gave the best mangrove discrimination with combination of Landsat 5 TM and ALOS. The OA achieved by RF classifier was 81.1% as compared to ML of 77% and 0.76 as compared to 0.71 for Kappa statistic.

From the research, RF algorithm gives best results using any of the layer combinations. Rodriguez-Giliano *et al*. (2015) describes RF as a powerful machine learning classifier that is relatively unknown in land RS, as compared to the traditional pattern recognition techniques. RF however provides an algorithm for estimating missing values, and the flexibility to perform several types of data analysis, that included regression, classification survival analysis and unsupervised learning.

In this research on the assessment of the usefulness of RF classifier for land- cover classification, the performance of the RF classifier for LULC classification was explored. Evaluation made, was based on mapping accuracy sensitivity to data set size and noise. Result showed that RF algorithm yielded accurate LULC with a 92% OA and had a Kappa index of 0.92.

2.10 Accuracy Assessment

Accuracy is measured as the degree of closeness of result to the true value. With the introduction of more advanced digital satellite RS imagery, carrying out of accuracy assessment has gained a heightened interest. Until recent times, many techniques simply presented accuracy with single number to give the accuracy of a classification. These accuracies were usually in no relation to the ground, locations which were totally ignored. These type of accuracies could result in very high accuracy which are usually misleading. Moreover most of the dataset used for the accuracy assessment are datasets used to train the data. There are now several methods used to determine accuracy assessment such as the variance analysis, minimum accuracy value used as an index of classification accuracy, spatial error and class attribute errors. The most common way to symbolise classification accuracy of remotely sensed data is in the form of an error matrix. The use of error matrix is recognized by most researchers as standard reporting convention (Congalton, 1991). It is the approach widely used in accuracy assessment (Foody, 2002b). With error matrix a square array of number is set out as rows and columns. These expressed as the error matrix can then be used as the beginning point for a series of descriptive and analytical statistical techniques. Perhaps the simplest descriptive statistic is overall accuracy which is calculated by dividing the total correct pixels by the total number of pixels in the error matrix.

Traditionally, the amount of correct pixels in a category is divided by the total number of pixels of that category as derivative of the reference data (i.e., the column total). This accuracy measure shows the probability of a reference pixel being correctly classified and is really a degree of omission error. This accuracy measure is known as producer's accuracy. The producer of the classification is interested in how well a certain area can be classified. Moreover, if the total number of correct pixels in a category is divided by the total number of pixels that were classified in that category, then this result is a measure of commission error.

This measure which is "user's accuracy" or reliability, is an indicative of the error matrix. This accuracy is an appropriate beginning for the probability that a pixel classified on the map and image actually signifies that category on the ground (Congalton, 1991). An error matrix is a suitable beginning for many analytical statistical techniques. This is especially true of the discrete multivariate techniques. After the generation of an error matrix, other accuracy assessments such as the overall accuracy, omission error, commission error, and the kappa coefficient is determined. The kappa coefficient is described as the measure of overall statistical agreement of an error matrix. Kappa is recognized as a good method for comparing the difference between various error matrices (Congalton, 1991; Smith *et al*. 1991, Foody, 2004a).

2.11 Forecasting of mangrove forest changes.

Vazquez *et al*. (2016) researched on the detection and projection of Forest Changes. In their research they used Markov Chain Model and CA to determine the changes that have occurred in the Mangrove forest and forecasted what will occur in 2028. Markov Chain Model is a stochastic process model that describes the probability of change from one state to another. This is achieved by generating a transition probability of which a land cover type based on the pixel changes from one time T_1 to another T_2. A matrix developed from this point which is known as the transition matrix is used to determine the predicted LULC for a future. The mathematical expressions of the transition probability are shown in Equation 1 and Equation 2.

$$\sum_{i=1}^{m} P_{ij} = 1_i = 1,2 \dots \dots \dots m \qquad \text{Equation (1)}$$

$$P = P_{IJ} = \begin{matrix} p_{11} & p_{11} \dots & p_{1m} \\ p_{21} & p_{12} & p_{2m} \\ p_{m1} & p_{m2} & p_{mm} \end{matrix} \qquad \text{Equation (2)}$$

P_{ij} is the probability of transition from a LULC to another, m is the type of land use of the area studied. P_{ij} usually ranges from 0-1. Combining Markov and CA-Markov allow for the

probability of transition to be geographically positioned. The CA-Markov Module which makes use of both the CA and the Markov Chain analysis was then used to predict the current year 2015. In the CA-Markov a continuity filter is applied to the transition area. This was then used to grow out land use from the second time to the later time at the same time assigning the spatial-weighting factor. Vazquez *et al*. (2016) also states that it is more realistic to determine short term projection rather than long term projections with the Markov chain analysis.

2.12 Summary

Mangrove trees are major contributor to marine environment. Mangrove swamps are unique ecological communities that serves as a link to freshwater and serves to host a rich diversity of animal species. Mangroves are well suitable for climate change mitigation, because they are known to be one of the best carbon sequesters. These sequestered carbon can be determined not only through destructive means but by taking field measurement and applying allometric equations to them. Mangrove forest ecosystem have received a greater recognition for the past few years because of their ability to sequester GHG. Various RS techniques have been applied to determining the aerial extent of mangrove through the use of various classification algorithm like maximum classifier, but RF is seen to be the best algorithm since RS data are discrete rather than continuous. Forecasting of mangrove forest can be achieved through the use of Markov Chain analysis and the application of CA-Markov which gives a more realistic projection on the short term rather than the long term.

CHAPTER 3 MATERIALS AND METHODS

3.1 Study Area

The study area is located at the mangrove site along the Amanzule River in Ellembelle in the Western region of Ghana (Figure 3.1). The study area covers an area of 1824.03 hectares.

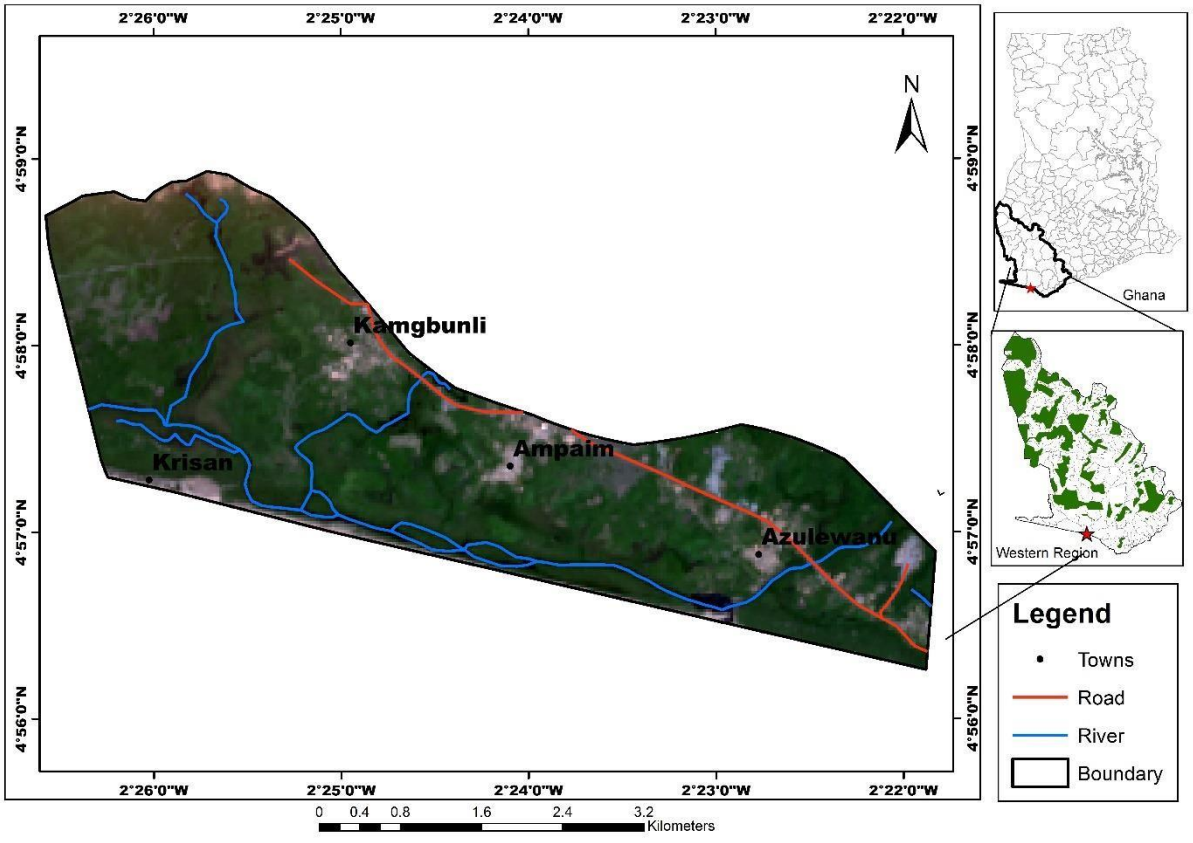

Figure 3.1: Study area

The area forms part of Greater Amanzule Wetland in the Nzema traditional area an important wetland ecosystems in Ghana. It is positioned within latitudes 4º56'0"N and 4º59'0"N, and between longitudes 2º21'40"W and 2º26'50"W. The mangrove forest is estuarine or riverine because it is found along the Amanzule River which meets the sea at Amanzule estuary.

Communities around the mangrove site are Ampaim, Krisan, Kamgbunli, Azulewanu. Although there are many benefits obtained from mangroves there are threats to the mangrove forest by both the indigenes and investors. The study area is not part of five chosen wetlands that are managed under the Ramsar Convention of 1975; Anlo – Keta lagoon complex, Densu delta, Muni Lagoon, Owabi, Sakumono 1 Lagoon, Songor Lagoon, they are only managed through indigenous systems.

3.1.1 Geology and Mineral

Rocks present there comprises of Cambrian type of the Birimean formation, Tarkwaian sandstone-Association, Quartzite and Phylites type. The presence of kaolin, silica and gold as well as sandstone deposit add an economic edge.

3.1.2 Relief and Drainage

The Amanzule River is found on the southern part of the district and the main river for the research study. Ankobra River is the major river found in the district. Major tributaries includes Ahama together with Nwini Rivers. Ankasa and Draw River forms boundary with Wassa Amenfi District.

3.1.3 Climate

The mean annual rainfall figures recorded in this area ranges from 26.8mm to 42.6mm which occurs in May and June. There are good sources of fishing and irrigation farming which provides employment. A high relative humidity record attained in this area ranges from 27.6% to 26.6% between May and June and 27.3% to 27.9% in the course of the year.

3.1.4 Vegetation Cover

The vegetation available here is the moist semi-deciduous rain forest and secondary forest in the northern and southern parts respectively. About 70km along the coastline is covered by savanna vegetation. The District is enriched with timber and non-timber like bamboos rattan and many others.

There are lots of forest reserves in the district. Shelter Forest Reserve, Draw River Forest Reserve and the Ndumfri Forest Reserve are all large reserves found in the Northern part of the district. The Amanzule River is located at the southern part of the district and surrounded by Mangrove forest. The Community Resource Management Area (CREMA) concept, by Wildlife Division of the Forestry Commission is to aid in putting limit to the unsustainable usage of natural resources. The district is endowed with rich variety of fauna and flora.

3.1.5 Nature of the soil

The soil type is ferric acrisols and dysric fluvisols. About 98% of the land is covered by ferric acrisols, this supports the cultivation of a wide range or variety of crops including cocoa, coffee, coconuts, oil palm, plantain and cassava. Due to this characteristic, the district has a comparative advantage in agriculture especially in the area of agro –processing and plantations.

3.1.6 State of the Natural Environment

The district is faced with many challenges. Prominent amongst these challenges are deforestation, bushfire, soil erosion and mining and quarrying. These factors are disturbing as their effect could lead to food insecurity and aggravation of poverty in the district.

Amongst their tracts of forest is the mangrove forest. However, the forests in this area are reported to record high occurrence of deforestation. This can be attributed to the exploitation of timber for logs and lumber by legal and illegal chainsaw operators. Mangroves are also reported to be deforested for firewood and construction purposes. They are also reported to be cleared to make way for fish farming and wood fuel.

3.2 Materials Description

3.2.1 Satellite Imagery

Multispectral images of Landsat 8 OLI/TIRS was obtained for the year 2015, Landsat 7 ETM+ for the year 2000 and Landsat 5 TM for the year 1991 were obtained from the US Geological Survey (USGS) Centre for Earth Resources Observation and Science (EROS), (USGS,2014). Data collected were within the same season of the years, the spatial resolution of the images were all of 30m. The research was based on a decadal analysis of images but due to lack of clear images of cloud cover less than 10%, the data obtained had difference of 9 years for 19912000 and from 2000-2015, 15years. The various bands of the images are explained for the type of Landsat imagery used in the Table 3.1.

Table 3. 1: Band and wavelength for Landsat 5, Landsat 7 and Landsat 8

	Landsat 4-5	Landsat 7	Landsat 8		Resolution
			Band 1 - Coastal aerosol	0.43 - 0.45	30
Band 1	0.45-0.52	0.45-0.52	Band 2 – Blue	0.45 - 0.51	30
Band 2	0.52-0.60	0.52-0.60	Band 3 – Green	0.53 - 0.59	30
Band 3	0.63-0.69	0.63-0.69	Band 4 – Red	0.64 - 0.67	30
Band 4	0.77-0.90	0.77-0.90	Band 5 - Near Infrared (NIR)	0.85 - 0.88	30
Band 5	1.55-1.75	1.55-1.75	Band 6 - SWIR 1	1.57 - 1.65	30
Band 6	10.40-12.50	10.40-12.50	Band 7 - SWIR 2	2.11 - 2.29	30
Band 7	2.09-2.35	2.09-2.35	Band 8 - Panchromatic	0.50 - 0.68	15
Band 8		0.52-0.90	Band 9 – Cirrus	1.36 - 1.38	30
			Band 10 - Thermal Infrared (TIRS) 1	10.60 - 11.19	100 * (30)
			Band 11 - Thermal Infrared (TIRS) 2	11.50 - 12.51	100 * (30

The list of instruments used for the field work are shown in Table 3.2. Table 3. 2: List of instruments used for the field work

Instrument	**Purpose of usage**
Handheld GPS Garmin Etrex	Navigation and picking of positional data
Diameter Tape	Diameter Measurement
Measuring tape 50 meters	Length of measurement
Field Datasheet	Recording field data

The software used for this study are listed in Table 3.3.

Table 3. 3: List of software used in the thesis

Software	**Purpose of usage**
ArcGIS Desktop	Mapping and GIS analysis
Erdas Imagine	Remote sensing and Image Processing
R	Classification
@Risk	Monte Carlo Simulation
Idrisi Kilimanjaro	Forecasting

The flowchart showing the sequence and method employed in embarking on the research is

shown in Figure 3.2.

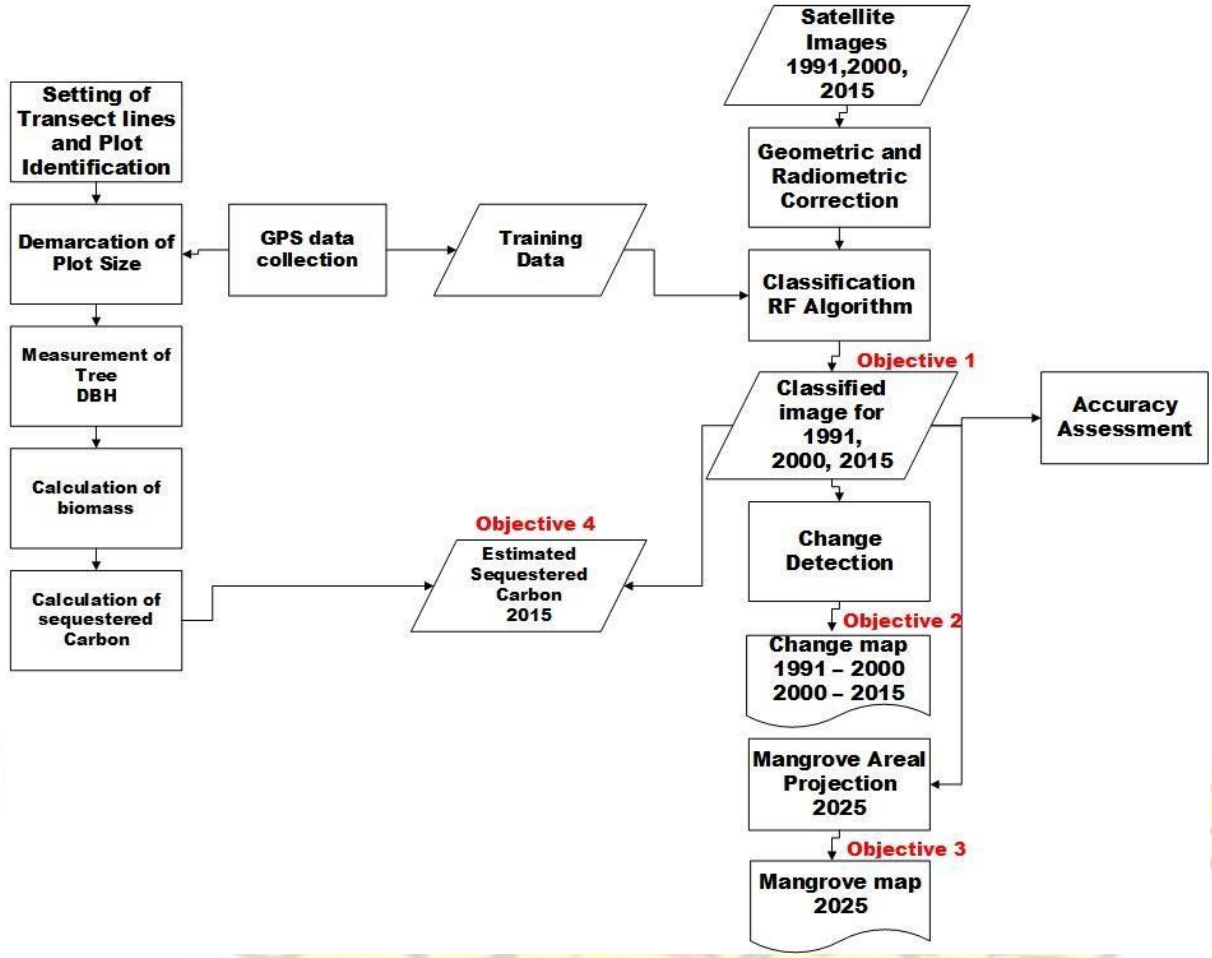

Figure 3.2: Flowchart of methodology

3.3 Field Work and Data collection

An extensive field work was carried out on the area of study, to measure the AGB of the study area. Location data were collected using a Garmin handheld GPS for training data and accuracy assessment. Google Earth Imagery were used for visual inspection. The GPS points collected were converted to KMZ format which is acceptable by Google Earth to enable the validation of the land cover. Based on the measurement, *in situ* data will be obtained and estimation of carbon stock can be made. Variety of information including positional and allometric measurement were collected. The data collected were relative to the adult, dead standing, dead

downed and juvenile mangroves. The data was collected along a transect line drawn within the area of study.

3.3.1 Transect Line

A transect line was made along the stretch of the study area. Due to the marshy grounds, accessibility to some part of the mangrove forest was not possible hence a uniformed distance for choosing sites along the transect line was not achieved. A distance of approximately 100meter was used in assigning plot location. Each plot was randomly selected and plotted into a 20m by 20 m (0.4ha). An inner plot of 5m by 5m (0.1ha) was created within the 20m by 20m. The 50 meter tape measure was used to measure out the plot. The positional location of the plot was taken to create Permanent Sample Plots (PSP) in order that the plots could easily be relocated and also plotted.

3.3.2 Data Collection for Adult Mangrove

Once the plots had been created, all the Mangrove trees found within the boundary of the 20m by 20m boundary were measured. Measurements were taken with a Diameter tape. The measurement of the biophysical parameters DBH measurement were taken and recorded as well as the canopy height of the mangrove forest. DBH Measurements were taken at 1.3m about ground level. Collection of the data was based on the available biomass, dead standing, dead downed and juvenile. The sampling species in each case were duly noted.

3.3.3 Data Collection of Dead Standing

Within the plot area of the data collection for the Adult mangrove, the same area was used in collecting the data for trees that were dead standing or dead and downed wood. The diameters for both the base and the tip were measured.

3.3.4 Data Collection for Juvenile Plants

Sampling juvenile mangroves within a plot were based on a sub-plot with dimension of 5 meter by 5 meter as shown in Figure 3.3.

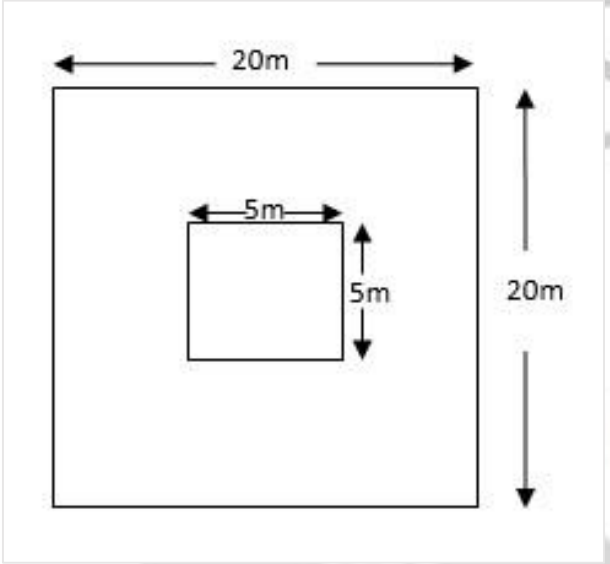

Figure 3.3: Plot dimension

3.3.5 Measuring Diameter

DBH was measured using a diameter tape. The diameter tape is calibrated in a way to convert the girth of the tree into its diameter, meaning that there was no need to recalculate and convert the reading taken into the DBH from the girth of the mangrove tree as a direct diameter reading is taken. Readings of the breast height of a tree was measured at 1.3m above the ground. Taping around the girth was done by stretching the tape firmly against the trunk. When abnormities such as the prop roots prevent a measurement from being taken an appropriate height was chosen by following the procedure shown in the Figure 3.4.

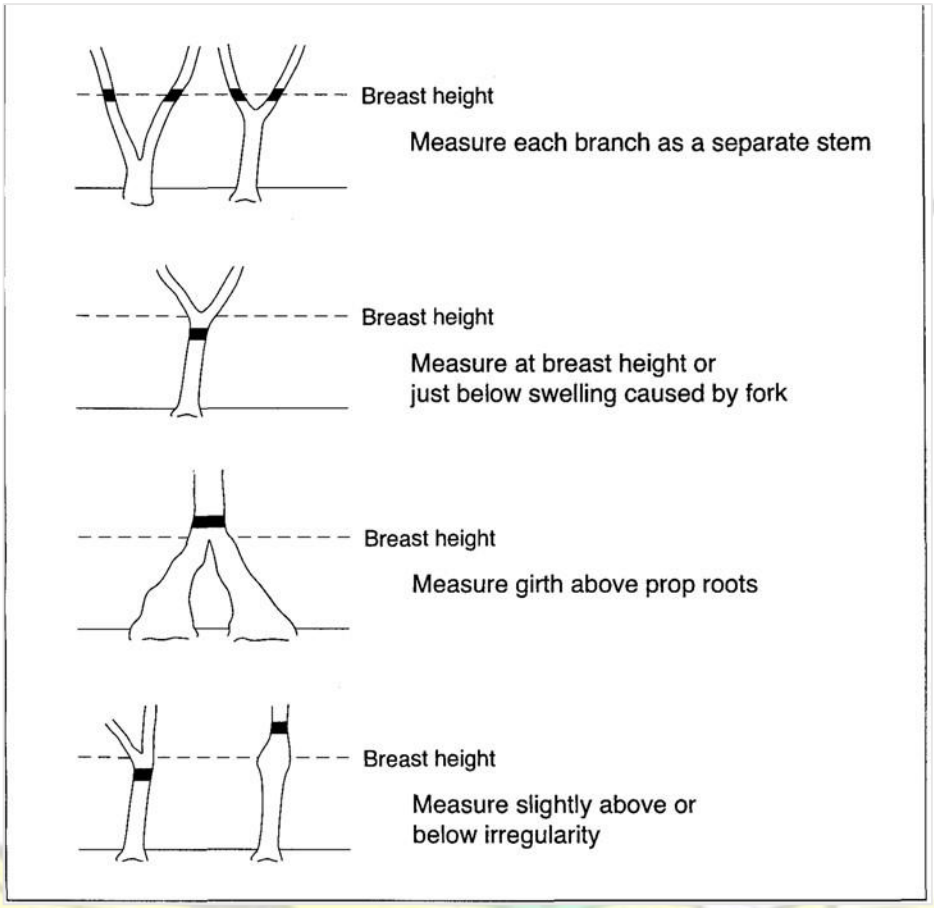

Figure 3.4: Method for measuring DBH on trees with unusual or different growth forms.

(Source: English *et al*., 1997)

In measuring, trees that props below 1.3m were measured separately as individual trees. Trees that propped above 1.3m was considered as a single tree. Trees with prop roots just below the breast height were also considered a single tree and measured as such. Trees with irregularity occurring at the breast height level were measured slightly above or below irregularity as shown in Figure 3.4.

3.4 Parameters used on the field data analysis

3.4.1 Determining Above Ground Biomass

The AGB was measured using the allometric equations. This was based on the tree DBH and density of the species of mangrove. The various allometric equations have been developed for mangrove by the CSIR and Forestry Commission of Ghana. Based on the calculated

parameters and models available, Equation 3 was used to determine the Above Ground Biomass.

$$AGB = a * p(D^2)^b \quad \text{Equation (3)}$$

Where AGB: is the above biomass per mangrove tree; a = 0.204, D: is the measured tree diameter at breast height; and ρ: wood density of the mangrove and b is 1.225

3.4.2 Calculating the Above Ground Carbon

The Above Ground Carbon (AGC) was determined by using Equation 4 after obtaining the above ground biomass in Tons/Hectare.

$$AGC = \left[\frac{\frac{AGB}{1000}}{Area} * \frac{1}{0.48}\right] \quad \text{Equation (4)}$$

Area = Plot size in hectares.

3.4.3 Determining Below Ground Biomass

The Below Ground Biomass (BGB) was measured using the allometric Equation 5. This was based on the tree diameter at breast height and density of the species of mangrove.

$$BGB = a * (AGB)^b \quad \text{Equations (5)}$$

Where BGB: is the above biomass per mangrove tree; a = 9.6404 and AGB is the above ground biomass and b= 0.2523

3.4.4 Calculating the Below Ground Carbon

The Above Ground carbon was determined by using the equation 6 below after obtaining the above ground biomass in Tons/Hectare

$$BGC = \left[\frac{\left(\frac{BGB}{1000}\right) * \left(\frac{1}{0.04}\right)}{0.48}\right] \quad \text{Equations (6)}$$

3.4.5 Standing Dead Wood

The Equation 7 was used to estimate volume of the wood and Equation 8 to determine the biomass.

$$Vol = \frac{1}{3}\pi h(\frac{{d_1}^2}{2} + \frac{{d_2}^2}{2} + \frac{d_2}{2} * \frac{d_2}{2}) \quad \text{Equation (7)}$$

Vol, is volume of truncated cone (cm^3), h is the height in cm, d_1 is the diameter at the diameter of the tree (cm) and d_2 is the diameter of the tree (cm). In the situation where there was no measurement to the top diameter of the bole, the value is treated as zero.

$$\text{AGB} = \text{Vol} * \rho * 0.001 \quad \text{Equation (8)}$$

Where AGB: is the dry biomass per mangrove tree; Vol is the calculated volume from Equation 7, ρ is wood density of the mangrove and 0.001 is a conversion factor to tons.

3.4.6 Dead Downed Wood

Calculation the volume of dead downed wood is shown by Equation 9 and above ground biomass is calculated with Equation 10.

$$Vol = \pi^2(\frac{{d_1}^2+{d_2}^2+{d_3}^2+{d_4}^2}{8L}) \quad \text{Equation (9)}$$

Vol is the volume of lying dead wood per unit area in density class plot (m^3h^{-1}), d1 is the diameter of piece of dead wood along the transect in plot (cm) and L is Length of the transect in plot (m)

$$AGB = \sum_{\rho}^{3} Vol_{plot,class} * Dens_{class} \quad \text{Equations (10)}$$

AGB is the above ground biomass of lying dead wood per unit area in plot (t dry matter ha^{-1}), Vol is volume of lying dead wood in density class in plot (m^3ha^{-1}), and ρ is wood density of the mangrove.

3.4.7 Total Carbon Stock

The Total Carbon Stock (TCS) or pool is estimated by adding all of the component pools. Each component pool was average across all plots. The average values were then summed to obtain the total.

3.4.8 Converting to Carbon Dioxide Equivalents

The total carbon density or total carbon stock was converted to Carbon Dioxide Equivalent (CO_2e) by multiplying carbon stock by 3.67. This is the ratio of molecular weights between carbon dioxide (44) and carbon (12).

3.4.9 Uncertainty in Component Pools

In determining the uncertainty in the component pools the 95% CI for each carbon pool (adult, juvenile, dead standing, dead downed) are used. Calculating for the total carbon stock requires accounting for uncertainty for each carbon pool. The equation for the uncertainty in the individual carbon pool is shown in Equation 11.

$$Uncertainty = 95\%CI\ half - width = (2 * SE) \quad \text{Equation (11)}$$

Where $SE = \frac{s}{\sqrt{n}}$(S is the standard deviation, n is the number of sample), CI is the confidence interval.

95%CI half-width was used to express the uncertainty as a percentage of the mean (Equation 12).

$$\text{Uncertainty (\%)} = 100 * \frac{(95\%\text{CI half}-\text{width})}{\text{mean}} \quad \text{Equation (12)}$$

The calculation of the uncertainty of the carbon stock at the stand level was based on Monte Carlo simulation. A normal distribution was selected with an iteration of 50000 for a one time simulation.

3.4.10 Estimation of Carbon Stock

Estimation of carbon stock was based on the plots selected for sampling of the population of mangroves. The total mangrove area was based on the mangrove area obtained from the classified image in 2015. This was calculated using the equation 13.

$$\text{Area} = \text{M} * Cm \quad \text{Equation (13)}$$

Area is the estimated land area for the entire study area, M= total mangrove area Cm is the total estimated carbon stock for the plots

Uncertainty around the Total carbon stock in the study area was calculated based on equation 14.

$$95\%\text{CI half} - \text{width for } = \text{CA}_\text{T} * \text{TCS} * \sqrt{(\frac{95\%CI_{C1}}{Area})^{+} \left(\frac{95\%CI_{C1}}{TCS}\right)}$$

Equation (14)

TCS is the mean standard level carbon stock of mangrove 95%CI = the uncertainty of each parameter (expressed as 95% CI half width).

3.5 Image Processing

The images obtained where stacked together and displayed in the false colour combination using bands 4, 3 and 2. The Landsat image was already in zone 30N of the Universal Transverse Mercator (UTM) coordinate system, using a WGS 84 datum and reference ellipsoid and all other data was put in the same coordinate system.

3.5.1 Image Pre – processing

The Landsat 8 and 7 ETM+ level 1G images were geometrically corrected products however georeferencing was applied to the 1991 image with a Root Mean Square Error (RMSE) of

±0.2000m. The Landsat image for 1991 had a shift in its positioning. The various bands of the images were stacked together. The satellite images were taken through radiometric and atmospheric corrections; all three images from 1991, 2000, and 2015 were converted from digital number to reflectance values using the TOA based on Equations 15 and 16.

$$L\lambda = ((Lmax_\lambda - Lmax_\lambda) - (QCALmax - QCALmin)) * (QCAL - QCALmin) - Lmin_\lambda$$

Equation (15)

$$P_\lambda = \frac{\pi * L_\lambda * d^2}{ESUN_\lambda * cos\theta_S}$$

Equation (16)

QCAL is DN, $Lmin_\lambda$ spectral radiance scales to QCALmin, $Lmax_\lambda$ is spectral radiance scales to QCALmax, QCALmin is the minimum quantized calibrated pixel value, QCALmax is the maximum quantized calibrated pixel value, d is the distance from the earth to the sun, $ESUN_\lambda$ is the mean solar exoatmospheric irradiance, and θs is the solar zenith angle. For Landsat 8 the Equation 17 was used to determine the TOA planetary reflectance.

$$P_\lambda = \frac{p^\lambda}{sin\theta_{SE}}$$

Equation (17)

Where P_λ is the TOA planetary reflectance, with correction for solar angle, and θ_{SE} is the local sun elevation angle. Subsetting was done on the processed images in RGB. This was done using the Area of Interest (AOI) of the study area on all three images.

3.5.2 Classification

Classification was carried out on the Landsat imagery to determine the land use land cover. The composite bands used represented false colour combination. Classification was done based on the RF classifier algorithm with R programming software. RF algorithm was chosen due to its top performing algorithm for data classification and regression. The stacked Landsat images of 6- bands, band 1, 2, 3, 4, 5 and 7 were imported in R Studio. The processes to the classification

were run separately for Landsat 5, Landsat 7 and Landsat 8. Each covering the study area for the years 1991, 2000 and 2015. The following packages were imported into R; rgdal, raster and caret. The Landsat images were imported as RasterBrick object using the brick function from the raster package. Images were imported as false colour composite RGB.

Based on the data picked from the study area, a set of training areas were depicted as polygon shapefiles storing the identity for each land cover type in a column in the attribute table. The pixel values in the training area for every band in the Landsat image was extracted and stored in a data frame along with its corresponding land cover class id. This was done to train and fit a RF model with a dataset. The process was possible using the train function from the Caret package. Table 3.4 shows the various land cover id assigned.

Table 3. 4: LULC Id and names

ID	Land cover categories
1	Mangrove
2	Other Vegetation
3	Waterbody
4	Settlement
5	Bareground

3.5.3 Change Detection

Output for the classified images for 1991, 2000 and 2015 from the classification were continuous layers with a double precision pixel type and a pixel depth of 64bit. 64 bit data types' supports decimal therefore making the values continuous and the process of change detection quite impossible because it works on discrete values. The classified images were copied as new raster by making a copy of the raster dataset and loading raster datasets into a raster catalogue. The new raster data output was still maintained as an imagine file and was taken to discrete raster images and the Bits were reduced to 8 bits unsigned. The pixel type was therefore converted to an 8_bit Unsigned data type. The values here supported only discrete values from 0 to 255.

The output classified data were converted to polygon to force the discrete values into a single layer. To avoid the error of data not being thematic, the polygons were left as not simplified. This was to make the edge of the polygon conform exactly to the input raster cell edges. This option when applied makes the conversion of the resulting polygon feature class back to a raster the same as the original raster.

A matrix parameter was used in the process of change detection. This enabled an output based on the classified images that indicated how the class values of the input files overlapped. The thematic layers of the 1991 classified vector was used as against the thematic layer of 2000 classified vector. The outputs of the changes were kept as raster image files, each having discrete histogram values. Measurements were made to the areal extent of the changes that had occurred.

3.6 Accuracy Assessment

Ground truth point data were collected to validate the changes that have occurred to assess the accuracy of the classification and also to determine the kappa of the classification. Each 8 _bit unsigned raster dataset for the classified images bore in its pixel the value of classified index, depicting the land cover. The point data were overlaid on each classified images and the classified value upon which the data fell was extracted. A comparison was made from the extracted pixel values bearing the land cover type as against the actual ground data. The differences were calculated and the percentage generated to depict the accuracy of the data. Accuracy assessment was carried out for each images and the Kappa coefficient was used to confirm the classification.

3.7 Change and Time series analysis on classified maps.

A Markovian process was used to determine the future of the LULC map which was determined from the classification based on the RF algorithm. The prediction of the LULC was modelled

based on the immediate prediction state of 2015. This was carried out using the Markov Chain Analysis. In using the Markov Chain Analysis, a probability matrix was developed showing the changes from time one to time two. It was upon this basis that the projection was carried out for 2025. The classified images of 1991 and 2000 were used in the Markov model to generate the transition areas and probabilities. The output for the transition were without spatial reference hence a CA-Markov was used to give spatial character to the model.

The CA-Markov module which makes use of both the CA-Markov and the Markov Chain analysis was used to predict the year 2015. This was done using transition area that was an output from Markov Chain. In the CA-Markov a continuity filter of 5 was applied to the transition area. This was then used to grow out land use from the second time to the later time at the same time assigning the spatial-weighting factor.

A 2015 predicted output was developed and then compared to the 2015 classified image and to have a good idea of the prediction accuracy. A model was then created from the two images to be applied to forecast to the year 2025 to give a LULC map of 2025.

CHAPTER 4 RESULTS AND DISCUSSIONS

4.1 Spatial extent of Mangrove Forest.

Classification was carried out on the Landsat images for the years 1991, 2000 and 2015. The result in Figure 4.1 shows the various LULC. The LULC were categorized under Mangroves: which comprises of all species of mangroves, Other vegetation which is made up of all kinds of vegetation including plantations, coconut trees, grass and shrubs with the exception of mangroves; Waterbody which covers only streams and rivers and other patches of water on the

surface of the ground; Settlement which is made up of buildings and roads; and Bareground which comprises of sea shore and dry land without any vegetation or human development.

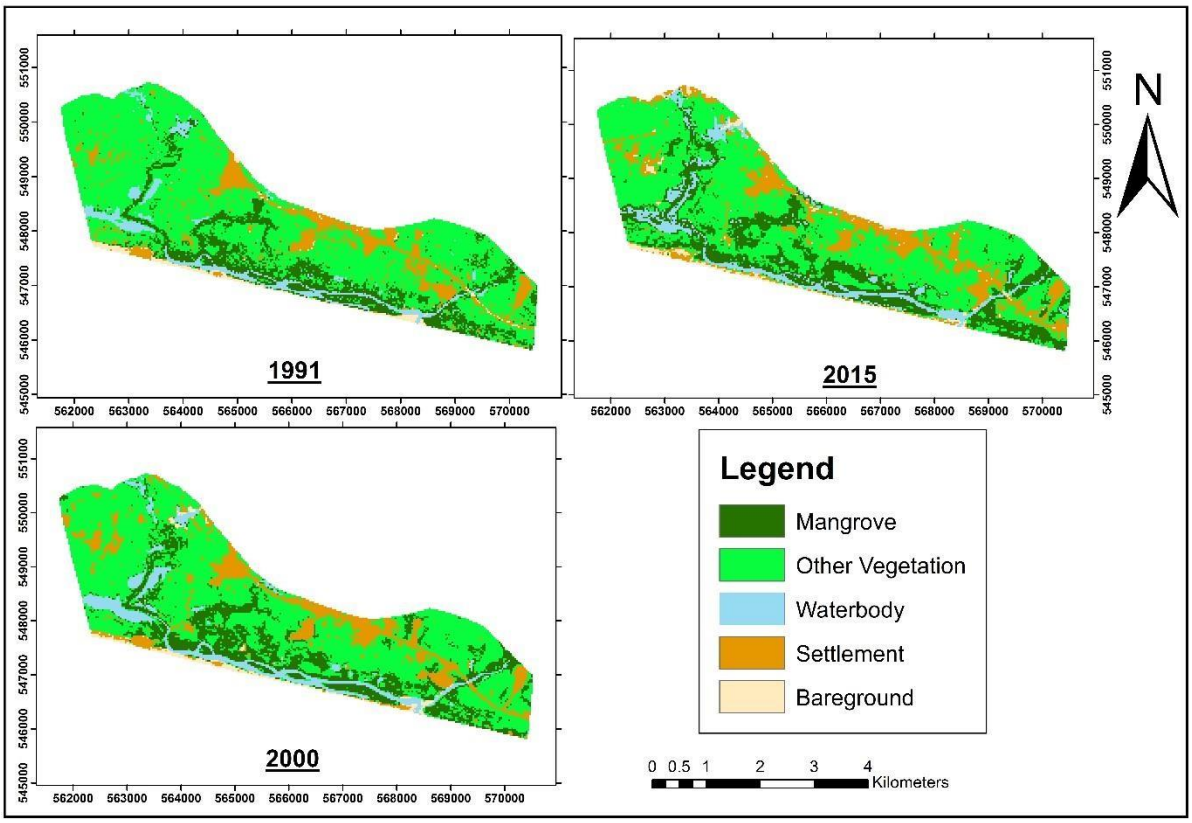

Figure 4.1: LULC map for 1991, 2000 and 2015.

The study area covers an area of 1824.03 ha. In 1991, about 298.35 ha representing 16.36% of the total area covered by mangrove increased significantly to 350.01 ha in the year 2000. The increment is about 19.19%. In the year 2015 there was a slight increase in the mangrove extent by 374.49ha (20.53%). The changes in other vegetation declined from 1991 through 2000 to 2015 by 1167.66 ha (64.02%), 1052.1 ha (57.68%) and 1009.89 ha (55.37%) respectively. In Ghana, REDD+ Readiness Preparation Proposal (R-PP) attributes the loss of Ghana's rich vegetation to institutional and policy-related factors. These includes activities such as smallscale agriculture, timber harvesting, land conversion and mining being the principal drivers. The continuous loss of Other vegetation can be attributed more to land conversion than to agricultural purposes. This is because dense vegetation including mangrove forests are often

cleared for farmlands and settlements (Forestry Commission, 2010). Waterbody, however showed increase in the year 2000 as compared to 1991 and 2015. In 2000 the extent of water was 5.91% that is 141.12 ha. In 1991, the extent is 7.74% that is 110.88 ha. In 2015 it decreased to 132.3ha (7.25%). Changes in Waterbody can be attributed to the twice - daily inundation of water in mangrove areas. This results in the overflow of the river causing the marshy ground and lots of water on the surface of the ground. As a result, Waterbody tends to increase or decrease depending on the day and time of capture (Gorczyca, 2014). An increasing trend is registered for settlement in the years 1991, 2000 and 2015 with 215.01 ha (11.79%), 242.55 ha (13.3%) and 261.99 ha (14.36%) respectively. There was an increase in the Bareground area in 1991, 2000 and 2015 respectively by 35.28 ha (1.93%), 38.25 ha (2.10%) and 45.36 ha (2.49%). Figure 4.2 is a chart showing the extent of changes in the classes. From the classified images, increase in Settlement and Bareground were generally seen around the main road and the townships, Krisan, Kamgbunli, Ampaim and Azulewanu. This is due to the increasing population and infrastructures. Settlement and Bareground in urban areas are the most increasing dynamic region on the earth surface resulting from tremendous increase in population and infrastructures (Galeon, 2008).

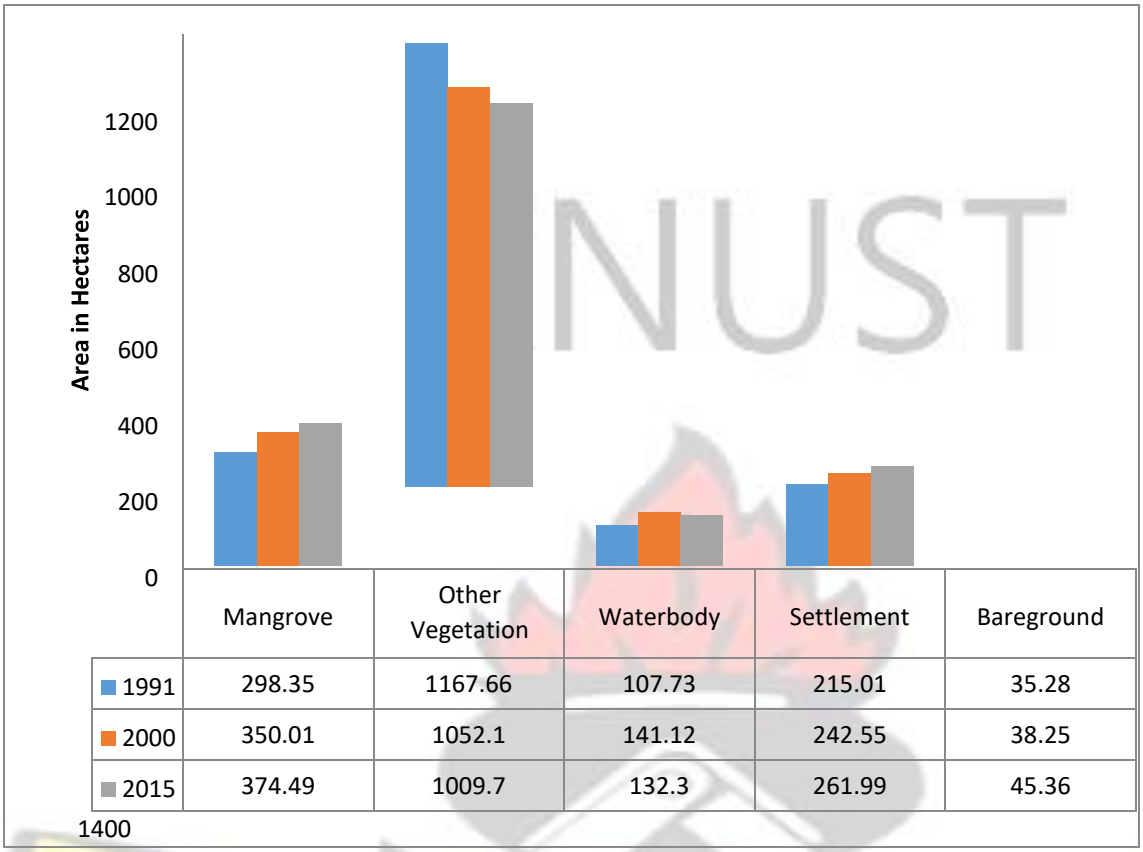

	Mangrove	Other Vegetation	Waterbody	Settlement	Bareground
1991	298.35	1167.66	107.73	215.01	35.28
2000	350.01	1052.1	141.12	242.55	38.25
2015	374.49	1009.7	132.3	261.99	45.36

Figure 4.2: A bar chart showing areas of LULC for the years 1991, 2000 and 2015.

The result from the classification of the satellite imageries indicates that mangrove is increasing despite the deforestation. Mangrove extent in 1991, 2000 and 2015 covered 298.35 ha, 350.01 ha and 374.49 ha respectively. Mangrove area increased from 1991 to 2000 and from 2000 to 2015 respectively by 51.66 ha and 24.48 ha. Analyzing the difference in the years from the images captured, it showed that within a nine year stretch (that is from 1991 to 2000) mangrove increased. Comparatively, the increase in the nine-year period is significantly higher than the increase in the fifteen years' period (that is from 2000 to 2015). Although mangrove was increasing, there was a decline in the rate of increase. This could have been shown more evidently with an additional data within the fifteen-year period for analysing rate of decline in mangrove. However, increase in mangrove can be attributed to the natural regenerative nature of mangrove to produce more seeds to fill the space of their disturbed canopy (Kauffman and Cole, 2010). Also the presence of afforestation projects and sensitization in the area by of the

indigenes as well as the sustainable management of mangrove education given by some nongovernmental organizations may have contributed to the increase in the mangrove forest.

4.2 Accuracy Assessment of LULC

The accuracy assessment based on the classified images showed an overall accuracy of 76.16% in 1991, with a kappa of 0.70. In 2000 the overall accuracy is 82.45% with a kappa of 0.78. The overall accuracy and kappa in 2015 are respectively 81.13% and 0.76.

The Kappa is the agreement between the model prediction and reality (Congalton, 1991). It is a better indicator of how the classifier performed across all instances. This is because a simple accuracy can be skewed if the class distribution is similarly skewed. Fleiss (1981) considers kappa greater than 0.75 as excellent and between 0.4 to 0.75 to be fairly good. The recorded kappa coefficients obtained for 1991, 2000 and 2015 were therefore good enough for the analysis.

4.3 Changes over the years

Changes from 1991 to 2000 in Table 4.1 shows that out of a total area of 298.35 ha covered by mangrove, 174.33 ha of the area retained the mangrove. Also 82.35 ha was converted to Other Vegetation. 30.15 ha covered by Mangrove changed to Waterbody, 5.67 ha of Mangroves changed to settlement and 5.85 ha also changed to Bareground. The bold figures indicates areas with changes.

Table 4.1: Area after change matrix on 1991-2000 LULC images.

2000 LULC

1991 LULC

	Mangrove	Other Vegetation	Waterbody	Settlement	Bareground	Column Total
Mangrove	**174.33**	82.35	30.15	5.67	5.85	298.35
Other Vegetation	157.77	**882.63**	30.6	92.7	3.96	1167.66
Waterbody	9.54	11.79	**78.93**	1.53	5.94	107.73
Settlement	7.74	74.43	0.18	**129.6**	3.06	215.01
Bareground	0.63	0.9	1.26	13.05	**19.44**	35.28
Row Total	350.01	1052.1	141.12	242.55	38.25	**1824.03**

There was, however, an increase in mangrove from 1991 to 2000 since 157.77 ha occupied by Other Vegetation changed to Mangrove. An area of 9.54 ha occupied by Waterbody gave way to Mangrove. Areas which were originally settlement and Bareground that gave way to Mangrove were 7.74 ha and 0.63 ha respectively. All these changes resulted in an increase in area occupied by mangrove resulting in the increase of the mangrove extent to 350.01 ha in 2000 (Figure 4.3).

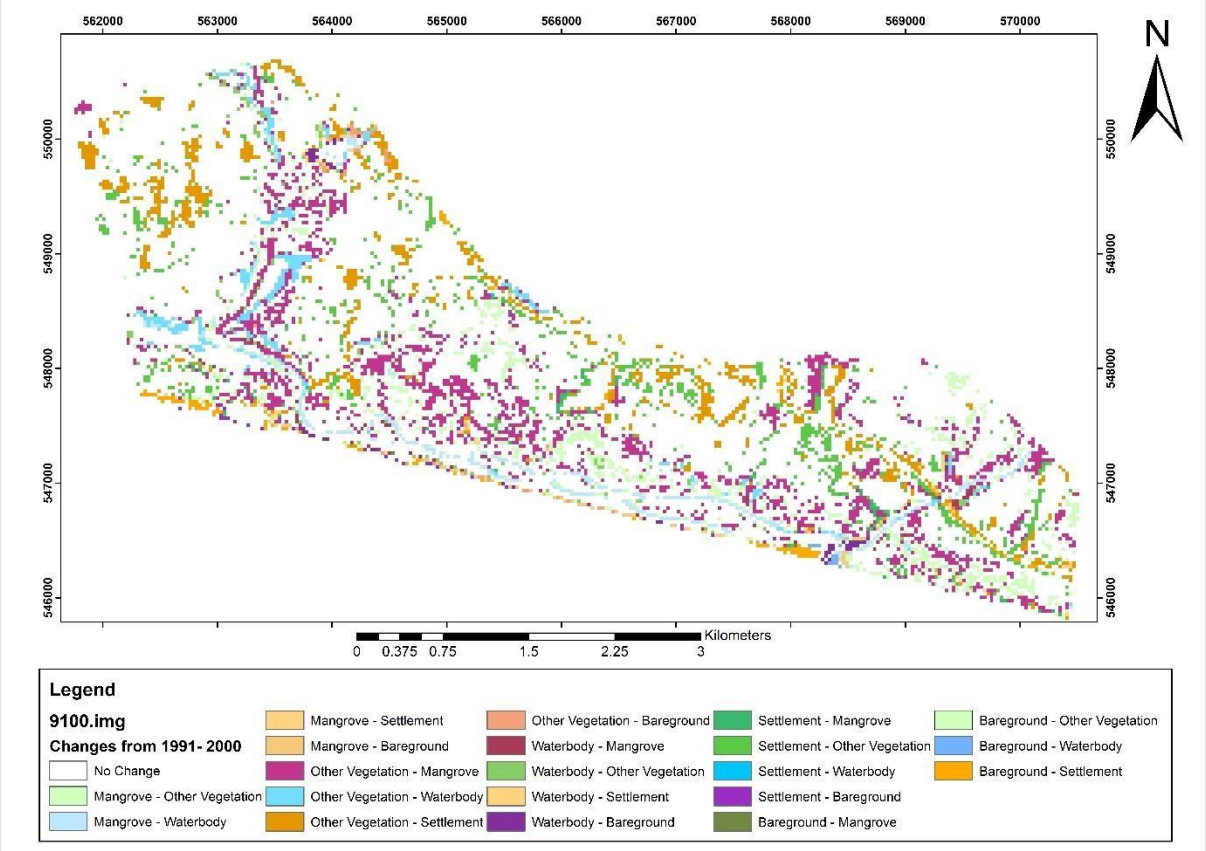

Figure 4.3: Change map showing LULC changes from 1991 to 2000.

Change map from 2000 to 2015 is shown in Figure 4.4. In Table 4.2, out of the 350.01 ha of Mangroves recorded in 2015, 214.74 ha still remained occupied with mangroves. The loss of mangrove cover to Other Vegetation, Waterbody, Settlement and Bareground and Other Vegetation Original mangrove are 114.39 ha, 14.31 ha, 5.22 ha and 1.35 ha respectively.

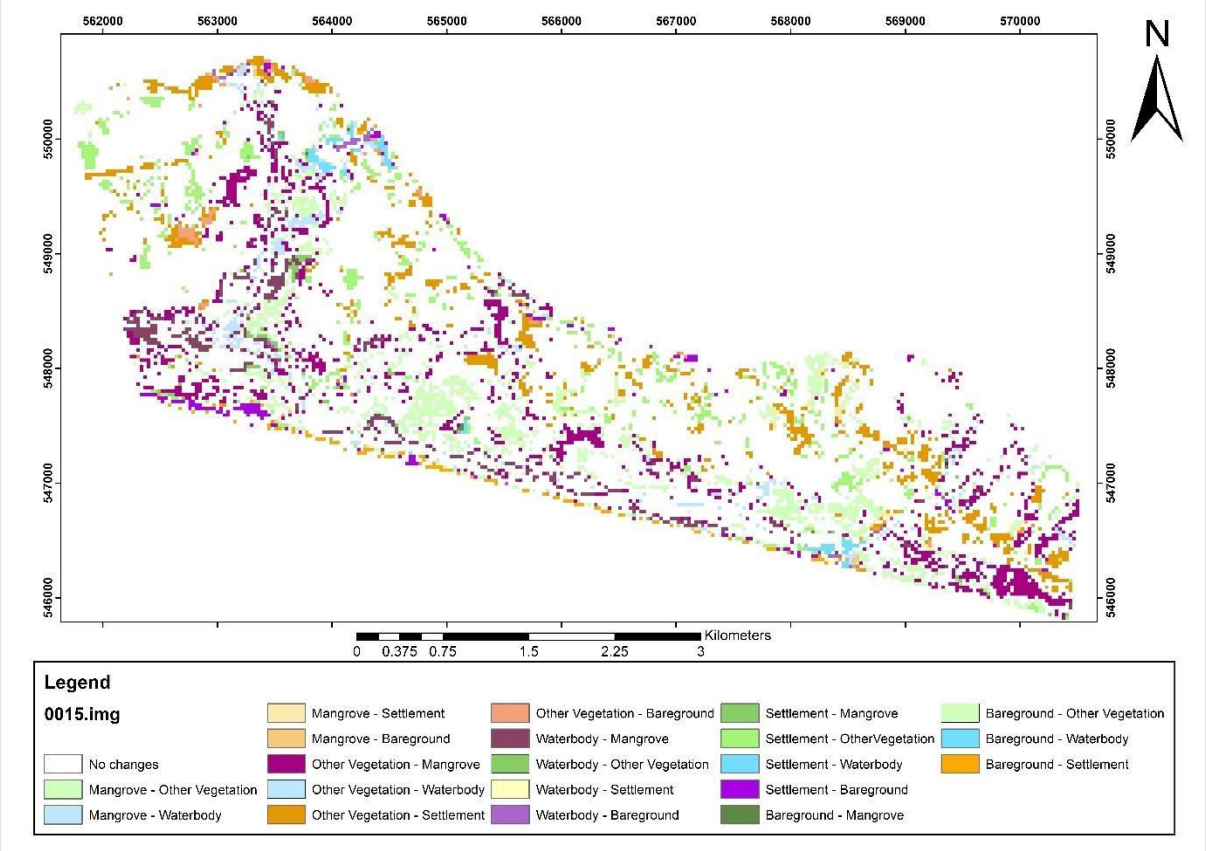

Figure 4.4: Change map showing LULC changes from 2000 to 2015.

The loss of Other Vegetation, Waterbody, Settlement and Bareground covers to mangrove 119.79 ha, 36.54 ha, 2.52 ha and 0.92 ha respectively. The total area covered by mangrove in 2015 showed that in spite of the changes, it increased to an area of 374.49 ha. Table 4.2 shows the tabulated change matrix from 2000-2015.

Table 4.2: Area after change matrix on 2000-2015 LULC images.

			2015 LULC			
	Mangrove	**Other Vegetation**	**Waterbody**	**Settlement**	**Bareground**	**Column Total**
Mangrove	**214.74**	114.39	14.31	5.22	1.35	350.01
Other Vegetation	119.79	**821.16**	13.86	89.1	8.19	1052.1
Waterbody	36.54	4.77	**95.22**		3.42	141.12
Settlement	2.52	66.51	1.62	1.17	**156.96** 14.94	242.55
Bareground	0.9	3.06	7.29	9.54	**17.46**	38.25

Row Total	374.49	1009.89	132.3	261.99	45.36	**1824.03**

From the results shown for the LULC maps, it is seen that although mangrove forest has increased over the years the increment is not uniform. Some areas have lost their mangrove cover whiles other areas have dense mangrove cover. Majority of the mangrove is lost to other vegetation. This can be attributed to the farming activities in the mangrove forest. From verbal interviews held with the indigenes around the mangroves sites, the mangroves especially the *Rhizophora mangle* were fell especially within the mangrove stretch in between Ampaim and Azulewanu for farming activities. The reason being that the *Rhizophora mangle* are good for smoking fish, because they give a better taste. Also, mangrove serves as firewood for cooking (Figure 4.5).

Figure 4.5: Rhizophora mangle tree for firewood

The indigenes also gave accounts of how they clear some areas in order to make way for shrimp and crab farming. The increase in mangrove especially in 2015 can be attributed to the afforestation of mangroves in the study area, especially in Ampaim (Figure 4.6).

Figure 4.6: Sprouting of afforested mangrove

According to the indigenes, some Non-Governmental Organisations have been sensitizing the community about the deforestation of mangrove therefore encouraging them not to cut down mangrove but rather to make use of the fallen dead mangrove trees. From the rate of increase in the mangrove forest for 2015 it is evident that not everyone is adhering to the advice. Moreover it can also be attributed to the fact that the sensitization programme is still at its early stages. *Rhizophora mangle* naturally occupies open spaces especially when their canopy is disturbed (Kauffman and Cole, 2010). Thus, the increase of mangrove in the study area can also be attributed to this phenomenon. Another factor that can contribute to the growth of mangrove is a result of the salinity of the river along the mangrove forest. Increase in salinity can affect the growth of the mangrove. (Kathiresan and Rajendran, 2005). Thus, there is need for further studies on the changes in salinity in the study area.

4.4 Predicted mangrove extent in 2025

The land-cover change was projected using Markov's transition probability matrices generated for the period 1991–2000. The transition matrices were verified by predicting for the land cover in 2015. The R^2 between the predicted results and the actual 2015 classification results is

0.9966 (Figure 4.7). The variation between the two datasets was small and the dependent variable can be predicted without error from the independent variable.

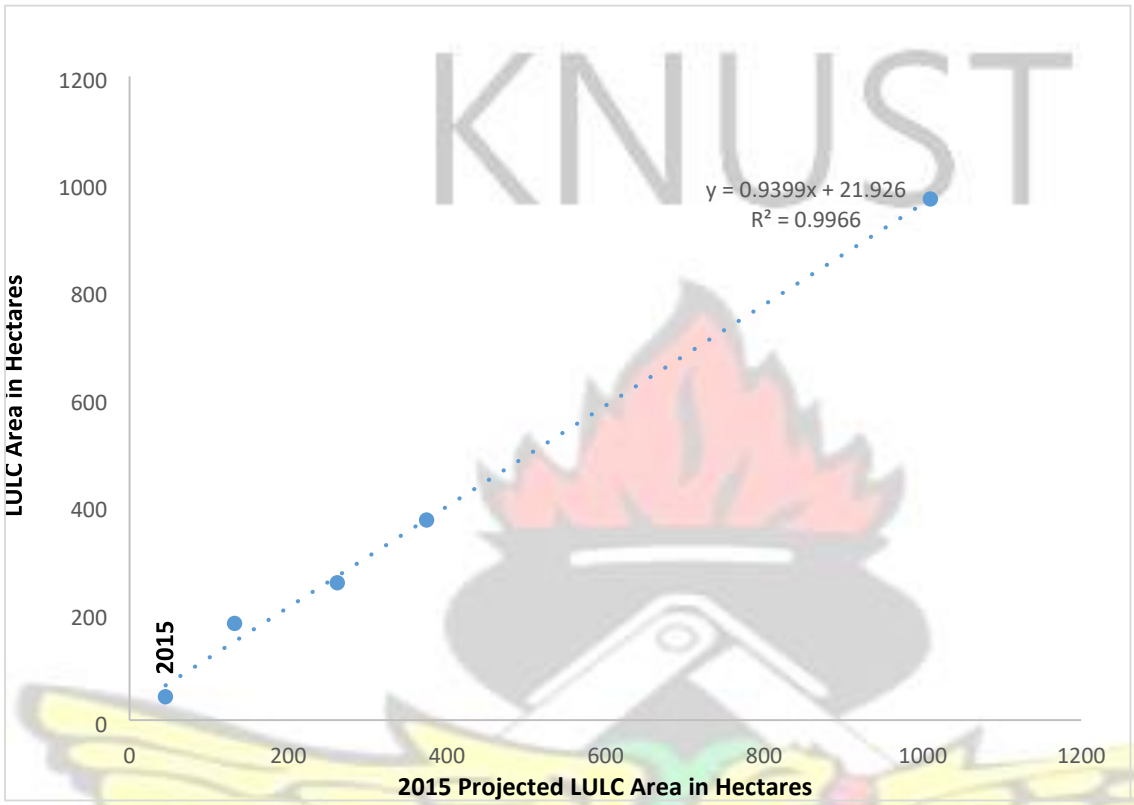

Figure 4.7: A linear equation showing correlation between 2015 LULC and 2015 projected LULC

This result showed that the transition matrices between 2000 and 2015 was effective in predicting land-cover for 2025. The 2025 image indicates that the area of mangrove forests increased from approximately 374.49 ha in 2015 to 381.69 ha in 2025. Figure 4.8 shows the predicted increase in the area covered by mangrove. Some areas, however, lost mangrove to other land cover types. This can be noted around the stretch between Amanzule and Ampaim. This can be attributed to the proximity of the settlement of Ampaim and Amanzule to the mangrove forest. Other vegetation decreased to 993.69 ha whiles Waterbody also decreased to 129.6 ha. Settlement and Bareground increased to 270.99 ha and 48.06 ha respectively (Table 4.3). This can be as a result of large population increase in the years. It can be anticipated that population will grow giving rise to more settlement and Bareground land cover types.

Table 4.3: Areal extent of LULC from 1991 to 2025

LULC	1991(ha)	2000(ha)	2015(ha)	2025 (ha)	
Mangrove	298.35	350.01	374.49	381.69	Total area 1824.03
Other Vegetation	1167.66	1052.1	1009.89	993.69	1824.03
Waterbody	107.73	141.12	132.3	129.6	1824.03
Settlement	215.01	242.55	261.99	270.99	1824.03
Bareground	35.28	38.25	45.36	48.06	

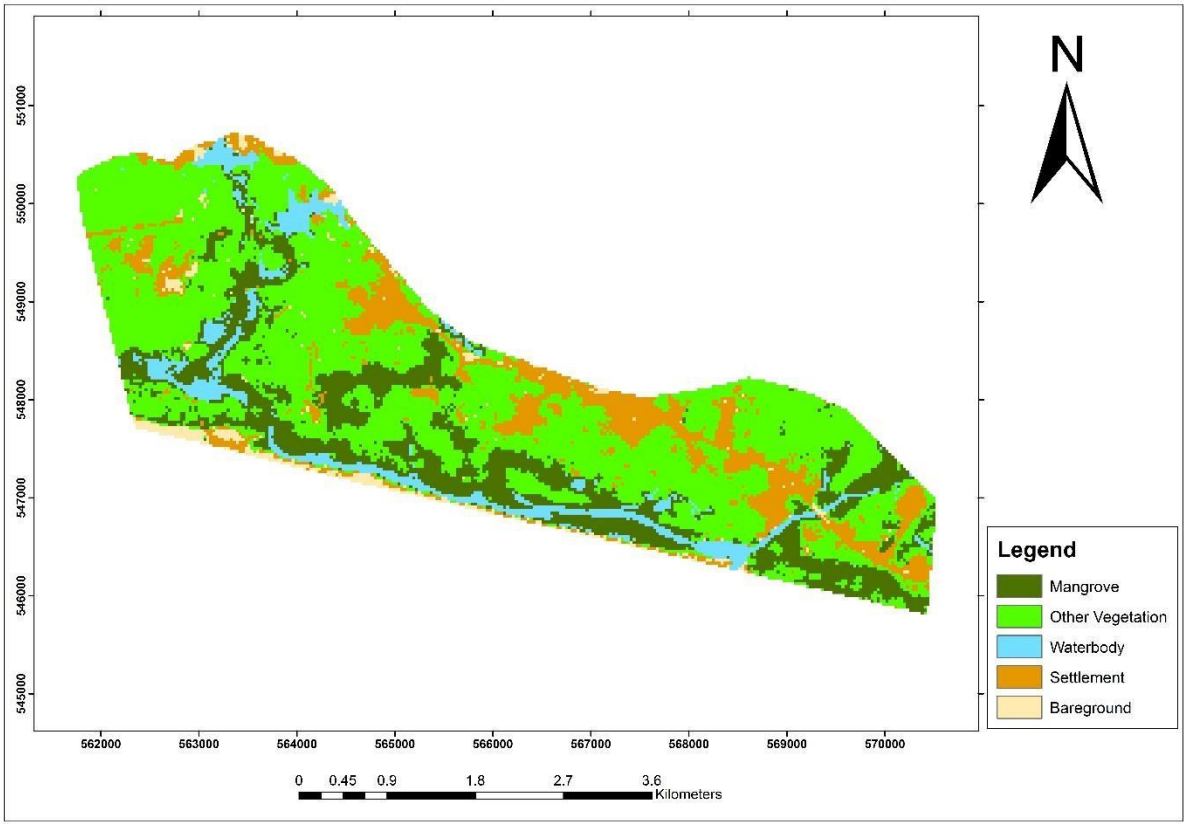

Figure 4.8: Projected LULC Map for 2025.

The projected classified image for 2025 shows an increase in the Mangrove extent; decrease in the Other vegetation and Waterbody; and an increase in Settlement and Bareground. From the result mangrove increased to 384. 64 ha. This shows that there will be an increase in mangrove of 7.7 ha more from 2015 and a significant decline in the rate of increment in mangrove forest. This means that although mangroves are seen to be increasing now, there is a high risk of losing the mangrove if mitigation procedures are not implemented. From the change map this result

showed that the transition matrices between 2000 and 2015 was effective in predicting landcover. The results indicate that the area of mangrove forests increased from approximately 374.49 ha in 2015 to 381.69 ha in 2025. Figure 4.8 shows the predicted increase in the area covered by mangrove. Some areas, however, lost mangrove to other landcover types. This can be noted around the stretch between Amanzule and Ampaim. This can be attributed to the proximity of the settlement of Ampaim and Amanzule to the mangrove forest. Other vegetation decreased to 993.69 ha whiles Waterbody also decreased to 129.6 ha. Settlement and Bareground increased to 270.99 ha and 48.06 respectively (Table 4.3). This can be as a result of large population increase in the years. It can be anticipated that population will grow giving rise to more settlement and Bareground land cover types.

There is a decline of Other vegetation. Thus, the vegetation is taking up the mangrove cover. This can be attributed to the increase in farmlands and felling of the mangroves along the river to make room for fishing activities.

4.5 Carbon Content in Mangrove

A total of 27 sites where selected along the transect line. The results obtained from the carbon sequestered in mangroves from each site is shown in Figure 4.9. Most of the sites were covered with *Rhizophora mangle*. Plot S is as mixture of red and white mangrove (*Laguncularia racemosa)* and dominant amongst all the plots are the *Rhizophora mangle*. Plot K recorded the highest sequestered Above Ground Carbon (AGC) of 10689.72 tons/ha and Below Ground Carbon (BGC) of 393.1255 tons/ha as against the Plot G which recorded the lowest AGC of about 6.979117 ha and BGC of 11.46096 tons/ha. Fewer mangroves were recorded within plots G resulting with an AGC of 6.98 tons/ha and 11.46 per ha of BGC. Mangrove in plot K, however, had the highest number of mangroves. The total carbon was converted to Carbon Dioxide Equivalent (CO_2e) by multiplying it with 3.67 which is the ratio of molecular weights

between carbon dioxide and carbon. A total of 38,139.7 tons for the AGB of all carbon pool was calculated and BGB also for all the carbon pool was 4,917.681 tons making a sum total of 43055.56 tons of Carbon.

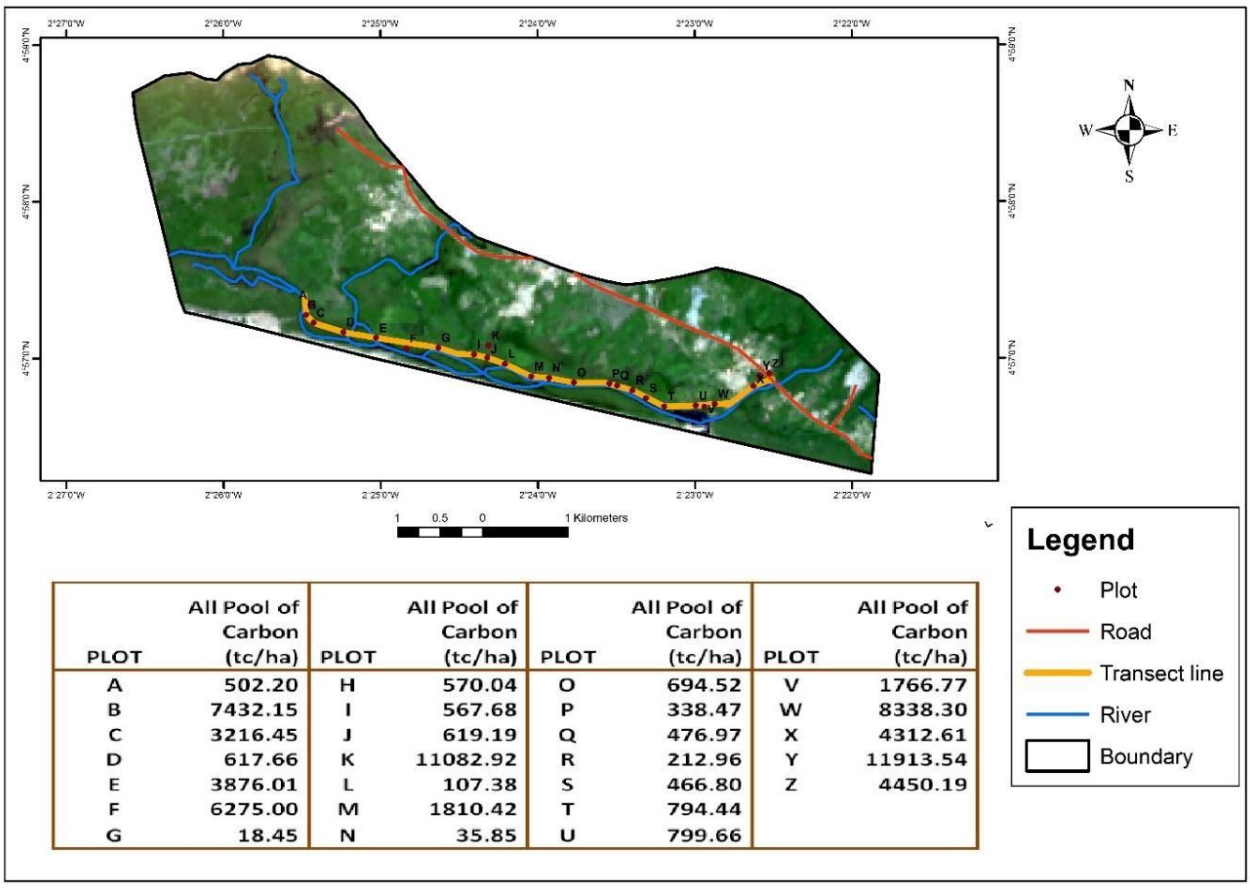

PLOT	All Pool of Carbon (tc/ha)	PLOT	All Pool of Carbon (tc/ha)	PLOT	All Pool of Carbon (tc/ha)	PLOT	All Pool of Carbon (tc/ha)
A	502.20	H	570.04	O	694.52	V	1766.77
B	7432.15	I	567.68	P	338.47	W	8338.30
C	3216.45	J	619.19	Q	476.97	X	4312.61
D	617.66	K	11082.92	R	212.96	Y	11913.54
E	3876.01	L	107.38	S	466.80	Z	4450.19
F	6275.00	M	1810.42	T	794.44		
G	18.45	N	35.85	U	799.66		

Figure 4.9: Carbon stock map of mangrove forest.

Using the Intercontinental Panel on Climate Change (IPCC) standard in tracking and predicting emissions of carbon from land cover change approach, the potential emissions that occurred with the mangrove was calculated. The carbon emission obtained from all the sites is 158,014 tons of CO_2e. The level of uncertainty obtained from individual carbon pool were large hence made it impossible to use the simple propagation of error. This is shown in Figure 4.10.

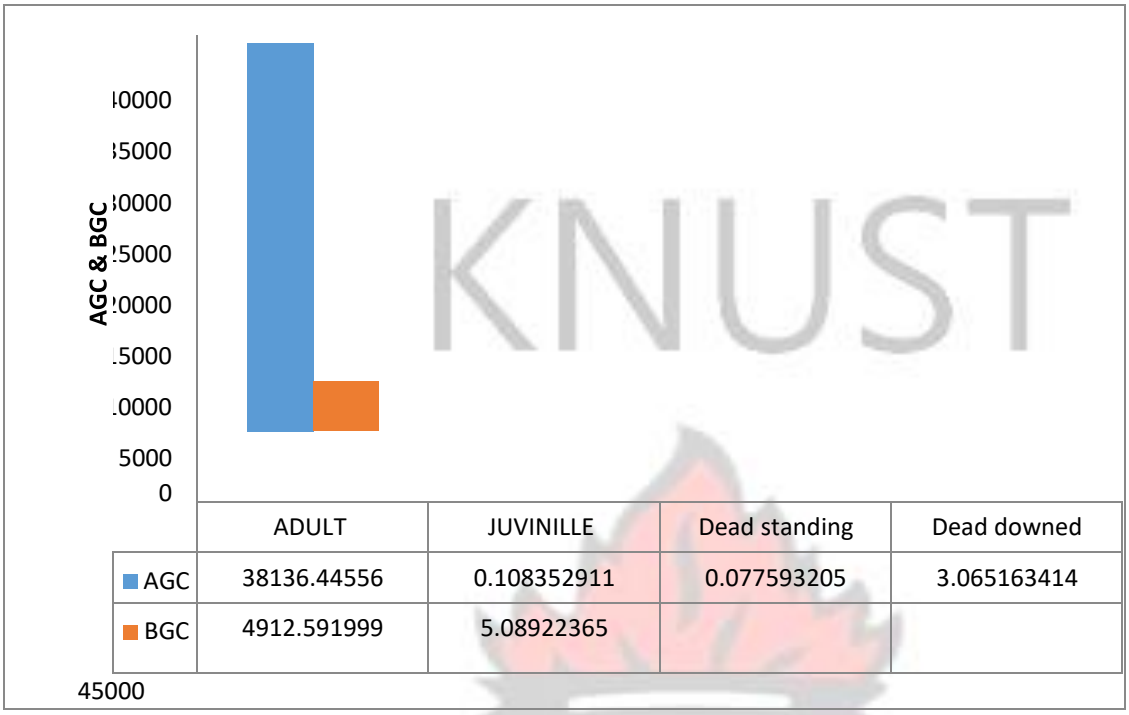

	ADULT	JUVINILLE	Dead standing	Dead downed
AGC	38136.44556	0.108352911	0.077593205	3.065163414
BGC	4912.591999	5.08922365		

Figure 4.10: Chart showing total above and below ground carbon

A Monte Carlo simulation of 50000 iterations was applied to the uncertainties to determine the uncertainty of the total stand level carbon stock (Figure 4.11).The uncertainty calculated at 95%CI was within the range of ± 152.55 ha^{-1} which falls within the acceptable 95%CI of ±1.53

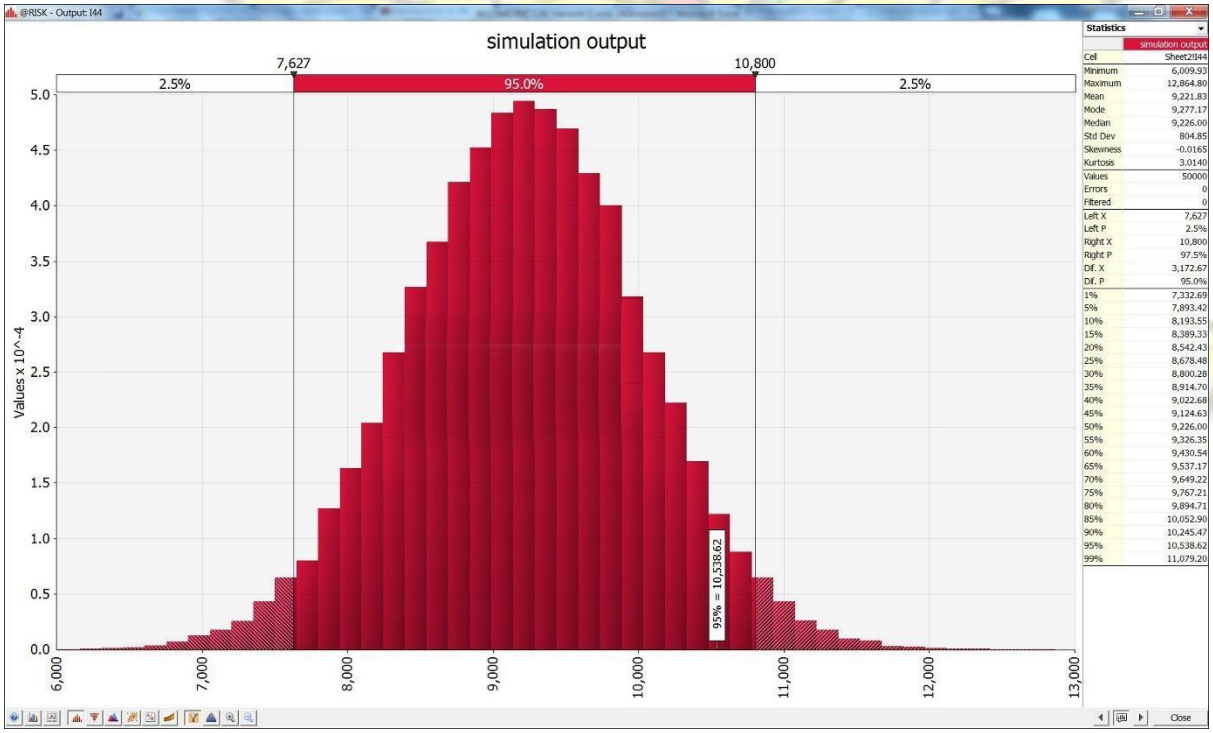

Figure 4.11: Simulation output of uncertainty for all the carbon pool.

Total carbon stock of the study area was estimated by finding the product of the carbon stock and the area of the study area. This gave a total of 1,550,295 tons with and uncertainty of ±57,125 tons. The results are shown in the Table 4.4.

Table 4. 4: Sequestered carbon in Mangrove from AGC and BGC.

	ADULT MANGROVE		JUVINILLE MANGROVE		Dead Standing	Dead downed	
PLOT	**AGC**	**BGC**	**AGC**	**BGC**	**AGC**	**BGC**	**overall Carbon**
A	338.3696	160.3945	0.070658		3.367897		502.2026
B	7064.71	366.8216			0.619471	7432.151	
C	2887.078	329.3722				3216.45	
D	457.2802	160.3773				617.6574	
E	3314.337	561.6769				3876.014	
F	5679.227	595.7749				6275.002	
G	6.979117	11.46096			0.010693	18.45077	
H	446.8494	120.8243	0.037695	1.721327		0.606302	570.039
I	446.8494	120.8243			0.009792	567.6835	
J	419.4985	199.6943				619.1928	
K	10689.72	393.1255			0.077593	11082.92	
L	83.85302	23.52662				107.3796	
M	1756.314	54.10233				1810.417	
N	29.13889	6.7136			35.85249		
O	536.8514	157.6721				694.5235	
P	220.5533	117.9149				338.4682	
Q	331.0674	145.9029				476.9703	
R	164.5711	48.3907				212.9619	
S	321.8661	144.9328			466.7989		
T	625.83	168.6083				794.4383	
U	612.24	187.4155				799.6556	
V	557.5796	180.2029				737.7825	
W	299.7717	184.103				483.8748	
X	242.5394	147.7103				390.2497	
Y	338.3696	160.3945				498.7641	
Z	265.0002	164.6547				429.6548	
Grand Total							**43055.56**
Mean	1466.786	188.9458	0.054176	2.544612	0.077593	0.311565	
StDev	2575.231	148.5882	0.023308	1.164301		0.347978	
	0.692	5.397334	0.077593		2577.545	1283.843	
Uncertainty			5220.768	111.1536			**±1.53**

Table 4.5 show the output for the parameters that gave the total carbon stock estimated for the mangrove area of in 2015. The area covered by mangrove was obtained from the classified image of 2015.

Table 4. 5: Table showing estimated carbon stock for the whole mangrove site

Parameters	**2015**
Total Mangrove Area	374.49
Total Area of carbon stock level ±152.55	4,139.97 uncertainty of Carbon Stock area per ha
carbon stock of the whole area **±57,125.4**	1,550,295.00 **Uncertainty of the whole area**

The study revealed that the carbon sequestered in each plot is relatively high, depending on the biomass sequestered at the plot. The carbon calculated for each plot is based on the AGB and the BGB, the dead downed wood and the dead standing. These do not give a comprehensive sum total of the carbon pool as the soil and litter were not considered a part of the carbon pool in this study. Most of the sampled plot had no juvenile plant recorded below 1cm DBH except for plots A and Plot H. The presence of dead standing is recorded only in Plot K and dead downed wood were recorded in Plots B, G, H and I. The absence of the dead downed wood and the dead standing wood can be attributed to the sensitization given to the people to make use of the dead downed and the dead standing biomass for firewood. It is therefore evident that with time there will be no dead downed woods and as such the living biomass will be the next option.

Plot G recorded the least AGC. This is due to less mangrove tree within the plot. The population of mangrove in plot K is more, giving an indication of high carbon in plot K. Plot K has rich mangrove stand with dense canopy. Mangrove in this section is bigger with average of 10cm DBH. Comparing Plot K to the other plots, it observed less disturbance as there were presence

of dead standing wood. This is because it is farther from the river. These contributed to the high Carbon obtained in Plot K. Again, it was observed that mangrove with DBH greater than 10cm sequesters more carbon.

The juvenile plants dead downed and the dead standing plants resulted in a higher uncertainty since the data collected per the plot size were few. Due to the large uncertainty, it was inappropriate to use a simple propagation of error to determine uncertainty of the carbon hence the use of the Monte Carlo simulation to normalize the uncertainty (Goslee *et al*., 2010). The summation of all the uncertainty of the carbon pool was used to simulate and determine the 95%CI of the data which was $\pm$1.53%. The common choice for confidence level was 95% and the level corresponded to percentage of area of the normal curve and the probability of observing a value outside the area is less than 0.05 (Goetz *et al*., 2009). This was because the normal curve obtained was symmetrical and half of the area was in the right side of the curve and the other half was in the left side of the curve. The CI gave an estimated range of values showing that the probability that the CI will contain the true parameter value for carbon, falls within the 95% CI.

CHAPTER 5 CONCLUSIONS AND RECOMMENDATIONS

5.1 Conclusions

The main of aim the research is to map out the mangrove area in the Ellembelle District and also to determine the carbon sequestered in mangroves. Based on the results on the formulated specific objectives, conclusions were drawn.

Objective 1: To map mangrove forest using RS and GIS.

Using RS and GIS, mangrove forest was mapped. The mangrove forest in the Ellembelle

District occupied an area of about 298.35 ha in 1991, 350.01 ha in 2000 and 374.49 ha in 2015. The mangrove forest stretches along the Amanzule River toward the Amanzule estuary. The mangrove forest was bounded closely by the following towns Azulewanu, Ampaim, Krisan and Kamgbunli.

Objective 2: To assess of mangrove forest change using RS.

The changes in the extent of mangrove forest over the period of 1991 to 2015 was realized from the LULCC map that mangrove forest is increasing. In 1991 mangrove occupied 298.35ha in 2000 it increased to 350.01 ha and 2015 it further increased to 374.49 ha. Although there are some degree of deforestation on mangrove, there have been some sensitization on the deforestation of mangrove which explains the increase in mangrove up to 2015. More satellite images within the gaps of the imagery would help understand better the frequency of change in the mangrove forest.

Objective 3: To predict the loss and gain of mangrove in the next decade, 2025.

In 2025 mangrove is expected to increase. From the forecasting carried out on the images, the results showed that mangrove will further increase to an extent of 381.69 ha in 2025. The increment of the mangrove forest depicts a declining trend from 1991 to 2025 indicating a potential risk if mitigation measure are not embarked upon. This requires monitoring of the mangrove forest both on the ground and with the use of RS imageries.

Objective 4: To determine the amount of sequestered carbon within the study area of mangrove above ground biomass, using a RS approach.

The total area occupied by mangrove in 2015 was 374.49 ha, it therefore gave an estimate of a total carbon stock of 1,550,294.566 tons and the equivalent carbon emission was 5,689,581.057 tons CO_2e. The uncertainty of the estimated carbon stock falls within $\pm$57,125.4. From the

results obtained, more sample plots and a complete assessment of the remaining carbon pools such as the litter and the soil will improve upon the estimated sequestered carbon. Nonetheless the research shows that the mangrove forest in the Ellembelle District sequesters a large amount of carbon and the availability of mangrove biomass carbon is helpful for the supervision of activities and also for the resilience of mangrove to changing environment.

5.2 Recommendations

From the conclusions of the research, the recommendations are enumerated below:

- Further research should be carried out on the BGB of the root, soil carbon and litter to understand the carbon sequestration over the entire mangrove ecosystem so that a full application for calculating the carbon stock can be utilized. BGB used in this research was based on the AGB calculated. Any error in the AGB could affect the BGB.
- Future carbon stock map could be refined with a well distributed plots evenly across the map.
- A continuous monitoring process should be adopted in the study area. As this will help in policy making and the creation of more effective educational programs among the indigenes which will discourage deforestation of mangroves and encourage afforestation of mangrove.

REFERENCES

Ajonina, G. (2011). *Rapid assessment of mangrove status and conditions for use to assess potential for marine payment for ecosystem services in Amanzule and surrounding areas in the western coastal region of Ghana, West Africa.* Washington DC.: The Marine Ecosystem Services (MARES) Program Forest Trends, 1050 Potomac Street, N.W. 1-24.

Bastiaanssen, W., Menenti, M., Feddes, R., & Holtslag, A. (1998). A Remote Sensing Surface Energy Balance Algorithm for Land - 1 formulation. *Journal of Hydrology*, 212213:198-212.

Berlanga-Robles, C., Ruiz-Luna, A., & Hernandez-Guzman, R. (2011). Impact of shrimp farming on mangrove forest and other coastal wetlands: The case of Mexico. In *Aquaculture and the Environment - A Shared Destiny Dr. Barbara Sladonja (Ed). ISBN 978-953-307-749-9* (pp. 18 - 28). Mexico.

Bouillon, S.; Borges, A. V.; Castaneda- Moya, E.; Diele, K.; Dittmar, T.; Duke, N.C.; Kristensen, S. Y.; Lee, C.; Marchand, J. J.; Middelburf, V. H.; Rivera- Monroy, T. J.; Smith, I. I.; Twilley, R. R.;. (2008). Mangrove production and carbon sinks: A revision of global Budget estimates. *Global Biogeochemical Cycles 22: GB2013, doi:10.1029/2007GB003052*, 1-12.

Breiman, L., & Cutler, A. (2004). *Random Forests.* Retrieved from https://www.stat.berkeley.edu/~breiman/RandomForests/cc_home.htm

Brieman, L. (2001). Random forest. *Machine Learning, Volume 45, Issue 1*, 5-42.

Chave, J; Andalo, C.; Brown, S.; Cairns, M. A.; Chambers, J. Q.; Eamus, D.; Folster, H.; Fromard, F.; Higuchi, N.; Kira, T.; Lescure, J.P.; Ogawa, H. P.; Ogawa, H.; Puig, H.;

Rifera, B.; Yamakura, T. (2005). The allometry and improved estimation of carbon stocks and balance in tropical forests Oecologia. 145,87-99.

Chen, C.-F., Son, N.-T., Chang , N.-B., Chen, C.-R., Thompson , C., & Aceituno, J. (2013). Multi-Decadal Mangrove Forest Change Detection and Prediction in Honduras, Central America, with Landsat Imagery and a Markov Chain Model. *Remote Sensing Volume 5, 6408-6426*.

Christensen, S., & Goudriaan, J. (1993). Deriving Light Interception and Biomass from Spectral Reflection ratio. *Remote Sensing Environment*, 39:141-152.

Cintron, G., Lugo, A. E., Pool, D. J., & Morris, G. (1978). Mangroves of arid environments in Puerto Rico and adjacent islands. *Biotropica 10*, 110-121.

Clough, B. F. (1998). Mangrove forest productivity and biomass accumulation in Hinchinbrook channel. *Mangroves and Salt Marshes 2*, 191-198.

Congalton, R. G. (1991). A review of assessing the accuracy of classification of Remotely Sensed data. *Remote Sensing Environment*, 35, 37.

Congalton, R., Oderwald, R., & Mead, R. (1983). Assessing Landsat classification accuracy using discrete multivariate analysis statistical techniques. *Photogrammetric Engineering and Remote Sensing*, 1671-1678.

Diop, E. S. (1993). Conservation and Sustainable Utilization of Mangrove Forests in Latin America and Africa Regions. Part II – Africa. International Society for Mangrove Ecosystems and Coastal marine Project of UNESCO. *Mangrove Ecosystems Technical Reports volume 3*.

Donato, D. C., Kauffman, B. J., Murdiyarso, D., Kurnianto, S., & Stidham, M. (2011). *Mangroves among the most carbon_rich forests in the tropics. Nature Geoscience: http://www.nature.com/naturegeoscience.* Retrieved from Nature Geoscience: http://www.nature.com/naturegeoscience.

Duarte, C., Middelburg, J., & Caraco, N. (2005). Major role of marine vegetation on the oceanic carbon cycle. *Biogeosciences, 2: 1–8.*

Elith, J., Leathwick, J. R., & Hastie, T. (2008). A working guide to boosted regression tree. *Journal of Animal Ecology*.

FAO. (2005). Global Forest Resources Assessment 2005, Thematic Study on Mangroves. *Forestry Department, Food and Agriculture Organization of the United Nations*, 1.

Fatoyinbo, T. E., & Simard, M. (2013). Height and biomass of mangroves in Africa from ICESat / GLAS and SRTM. *International Journal of Remote Sensing*, 668-678.

Fleiss, J. L. (1981). *Statistical method for rates and proportions.* New York: John Wiley, pp 200-204.

Foody, G. M. (2004a). Thematic comparison: evaluating the statistical significance of differences in classification accuracy. *Photogrammetric Engineering and Remote Sensing, 70*, 627-630.

Foody, G. M. (2004b). Superviesed image classification by MLP and RBF neural networks with and without an exhaustively defined set of classes. *International Journal of Remote Sensing*, 799.

Forestry Commission of Ghana. (2010). Ghana R-PP (Annexes).

Galeon, F. A. (2008). Estimating of population in informal settlement communities using high resolution satelliet image. *University of the Philippines, Dilima*, 1.

Giesen, W., Wulffraat, S., Zieren, M., & Scholten, L. (2007). *Mangrove guidebook for Southeast Asia. Food and Agricultural Organisation and Wetlands International.* Bangkok, Thailand: 1-193.

Gitahiga, M. N. (2013). *Structure and biomass accumulation of natural mangrove forest at Gazi Bay, Kenya.* Kenya: Kenyatta University, 20-60.

Goetz, S. J., Laporte, N. T., Johns, T., Walker, W., Kellndorfer, J., Houghton, R. A., & Sun, M. (2009). Mapping and monitoring carbon stocks with satellite observations: a comparison of methods. Carbon Balance and Management. 2-6.

GOFC-GOLD. (2011). *A sourcebook of methods and procedures for monitoring and reporting anthropogenic green house gas emission and removals caused by deforestation , gains and losses of carbon stocks in forests remaining forests, and forestation.* Alberta, Canada: GOFC-GOLD Report version COP17-1, GOFC-GOLD Project Office, Natural Resources Canada,1-243.

Gorczyca, K. (2014). Threats to Coastal and Marine Ecosystems. The ASEAN Member S . *Biodiversity: Value of Ecosystems.*, 1.

Gordon, C., & Ayivor, J. (2003). Report on the Africa Regional Workshop on the Sustainable Management of Mangrove Forest Ecosystems. *Workshop on sustainable management of Mangrove Forest Ecosystems*. Washington, DC: ISME.

Goslee, K., Walker, S. M., Grais, A., Murray, L., Casarim , F., & Brown, S. (2010). *Leaf Technicial Guidance Series for the development of a forest carbon monitoring system for REDD+: Module C-CS: Calculations for Estimating Carbon Stocks.* Winrock International.

Green, E. P., Clark, C. D., Mumby, P. J., Edwards, A. J., & Ellis, A. C. (1998). Remote Sensing Techniques for Mangrove Mapping. *International Journal of Remote Sensing , 19 (5), 935_ 956*.

Heumann, B. W. (2011). Satellite Remote Sensing of mangrove forests: Recent advances and future opportunities . Progress in Physical Geography. *Progress in Physical Geography* , 35, 87-108.

Horning, N. (2010). Random Forests: An algorithm for image classification and generation of continous field data sets. *International Conference on Geoinformatics for Spatial Infrastructure Development in Earth and Allied Science.* 1-4.

Jhonnerie, R., Siregar, P. V., Nababan , B., Prasetyo, L. B., & Wouthuyzen , S. (2015). Random forest classification for mangrove land cover mapping using Landsat 5 TM and ALOS PALSAR imageries . *The 1st International Symposium on LAPAN-IPB Satellite for Food Security and Environmental Monitoring* , 1,7.

Kathiresan , K., & Qasim, S. Z. (2005). *Biodiversity in mangrove ecosystems.* New Delhi: Hindustan Publishers,251.

Kathiresan, K., & Rajendran, N. (2005). Coastal mangrove forest mitigated tsunami. *Estuarine Coastal Shelf Science*, 601-605.

Kauffman , J. B., & Donato, D. C. (2012). *Protocols for the measurement , monitoring and reporting of structure, biomass and carbon stock in mangrove forests. Working paper 86.* CIFOR, Bogor, Indonesia: 1-36.

Kauffman, J. B., & Cole, T. (2010). Micronesian mangrove forest structure and tree response to a severe typhoon. *Wetlands 30*, 1077-1084.

Komiyama, A., Poungparn, S., & Kato, S. (2005). Common allometric equations for estimating the tree weight of mangroves. *Journal of Tropical Ecological 21*, 471-477.

Kuenzer, C., Bluemel, A., Gebhardt, S., Quoc, T., & Dech, S. (2011). Remote sensing of Mangrove Ecosystems: A Review. *Remote Sensing*, 875-915.

MacDicken, K. (1998). *A guide to monitoring Carbon Storage in Forestry and Agroforestry projects.* Winrock International, 5-80.

Mensah, J. (2013). Remote sensing application for mangrove mapping in the Ellembelle District in Ghana. USAID Integrated Coastal and Fisheries Governance Program for the Western Region of Ghana. Narragansett RI: Coastal Resources Centre, Graduate School of Oceanography,. *University of Rhode Island, United States of America.*, 1-24.

Mitch, W. J., & Gosselink, J. G. (2007). *Wetlands (Fourth).* New York USA: John Wiley and Sons, Inc. 7-70.

Mukherjee, A. (2007). Workable strategies in a coastal wetland ecosystem in sequestering carbon directly by geologic repositories and phytoplankton fertiliztion, ecosystem diversity and carbon sequestration challenges and a way tfor ushering in a sustainable futre. 551-554.

Nellemann, C., Corcoran, E., Duarte, C. M., Valdes, L., De Young, C., Fonseca, L., & Grimsditch , G. (2009). Blue Carbon. A Rapid Response Assessment. *United Nations Environment Programme. Norway: Birkeland Trykkeri AS, Norway*, 9-27.

NOAA. (2016, May 31). *NOAA Habitat Conservation | Coastal Blue Carbon.* Retrieved from http://www.habitat.noaa.gov/coastalcarbonsequestration.html.

Ong, J. E., Gong, W. K., & Wong, C. H. (2004). Allometry and partitioning of the mangrove, Rhizophora apiculata. *Forest Ecological Management.* , 395-408.

Pearson , T. R., & Brown, S. (2007). *Measurement guidelines for the sequestration of forest carbon. General Technical Report- NRS- 18, USDA Forest Service, Northern Research Station Newton Square, USA.* 1-47.

Pearson , T. R., Walker, S., & Brown, S. (2005). *Sourcebook for land use, land - use change and forestry projects. Report from BioCF and Winrock International.* Retrieved from http://www. winrock. org / ecosytems/ tools.app? BU = 9086 World Bank, Washington DC.

Richardson, J., Everit , J. H., & Gausman, H. W. (1983). Radiometric estimation of Biomass and N-content of Alicia Grass. *Remote Sensing Environment*, 179-180.

Rodriguez- Galiano, V. F., Ghimire, B., Chica-Olmo, M., & Rigol- Sanchez, J. P. (2011). An assessment of the effectiveness of a random forest classifier for land cover classification. *ISPRS Journal of Photogrammetry and Remote Sensing*, 93-104.

Saenger, P., & Snedaker, S. C. (1993). Pantropical trends in mangrove above-ground biomass and annual litterfall. *Oecologia 96*, 293-299.

Sellers, P. J., Meeson, F. G., Hall, G., Asrar, R. E., Murphy, R. A., Schiffer, F., . . . Schimel, P. D. (1995). Remote Sensing of the land surface for studies of global change : Models - Algorithms - Experiments. *Remote Sensing Environment 51*, 3 -26.

Smith , P. C., Dellepiane, S. G., & Schowengerdt, R. A. (1999). Quality assessment of image classification algorithms for land-cover mapping : a review and a proposal for a cost based approach. *International Journal of Remote Sensing 20*, 1461-1486.

Spalding, M., Kainuma, M., & Collins, L. (2012). World atlas of mangrove. *Routledge*, 1 - 3.

Tomlinson, B. P. (1999). The Botany of mangroves.Cambridge Tropical Biology Series. *Cambridge University Press*, 419.

Tripathi, S., Soni, K. S., Maurya, K. A., & Soni, K. P. (2010). *Calculating Carbon sequestration using remote sensing and GIS.* Retrieved from http://geospatialmedia.net

Trumper, K. M., Bertzky, M., Dickson, B., Van der Heijden, G., Jenkins, M., & Manning, P. (2009). The Natural Fix? The role of ecosystems in climate change. A UNEP rapid response assessment. UNEPWCMC. Cambridge, UK: 65p.

Tucker, C. J. (1979). Red and Photographic Infrared Linear Combination for Monitoring Vegetation. *Elsevier North Holland Inc. 8:127-150.*

UNEP. (2007). Mangroves of Western and Central Africa. *UNEP - Regional Seas Programme/ UNEPWCMC*, 92.

USGS, Earth Explorer. (2014). *USGS.* Retrieved from http://earthexplorer.usgs.gov/

Vaiphasa, C. (2006). *Remote Sensing Techniques for mangrove mapping.* Retrieved from https://www.itc.nl/library/Papers_2006/phd/vaiphasa_abstract.pdf

Valiela, L., Bowen, J. L., & Cork, J. K. (2001). Mangrove forests: One of the world's threatened major tropical environments. *Bioscience 51: 807–815*.

Vázquez-Quintero, G., Solís-Moreno, R., Pompa-García, M., Villarreal-Guerrero, F., PinedoAlvarez, C., & Pinedo-Alvarez, A. (2016). Detection and Projection of Forest Changes by Using the Markov Chain Model and Cellular Automata. *Sustainabiliy*, 8, 236.

Waran, M. A. (2001). Carbon sequestration potential of trees in and around Pune city. *Department of Environment Sciences, University of Pune*, 1 - 31.

Wojick, D. E. (1999). *Carbon storage in soils: The ultimate no-regrets policy? A Report to greening earth society.* Retrieved from Greening Earth Society: http://www.greening earth society.org/pdf/carbon.pdf.

APPENDIX

1. Plot Coordinates

PLOT	Longitude	Latitude
A	-2.42416	4.955681
B	-2.42458	4.95462
C	-2.42382	4.953769
D	-2.42065	4.952786
E	-2.41719	4.95217
F	-2.41394	4.951035
G	-2.41056	4.951121
I	-2.40678	4.9504
J	-2.40538	4.950055
K	-2.40527	4.95133
L	-2.40351	4.94938
M	-2.40071	4.948054
N	-2.39884	4.947886
O	-2.39619	4.947406
P	-2.39245	4.947285
Q	-2.39162	4.947069
R	-2.38999	4.946574
S	-2.38855	4.94571
T	-2.38662	4.944846
U	-2.38327	4.944932
V	-2.38236	4.944817
W	-2.38126	4.945123
X	-2.37716	4.947023
Y	-2.37651	4.948094
Z	-2.37549	4.948363

Accuracy Assessment for 1991

	Mangrove	Other Vegetation	Waterbody	Settlement	Bareground	Classification Overall	Producers Accuracy Precision
Mangrove	51	16	3	0	0	70	**72.86%**
Other Vegetation	1	42	0	2	0	45	**93.33%**
Waterbody	8	7	31	0	0	46	**67.39%**
Settlement	1	11	3	70	5	90	**77.78%**
Bareground	5	3	2	5	36	51	**70.59%**
Truth Overall	66	79	39	77	44	302	
User Accuracy (Recall)	**77.27%**	**53.17%**	**79.49%**	**90.91**	**87.81%**		
Overall Accuracy(OA)	**76.16%**						
Kappa	**0.7**						

Accuracy Assessment for 2000

	Mangrove	Other Vegetation	Waterbody	Settlement	Bareground	Classification Overall	Producers Accuracy Precision
Mangrove	59	7	4	1	0	71	**83.10%**
Other Vegetation	3	40	0	2	0	45	**88.89%**
Waterbody	6	0	40	1	0	47	**85.11%**
Settlement	1	4	3	77	7	92	**83.70%**
Bareground	0	2	2	10	33	47	**70.21%**
Truth Overall	69	53	49	91	40	302	
User Accuracy (Recall)	**85.51%**	**75.47%**	**81.63%**	**84.62**	**82.5%**		
Overall Accuracy(OA)	**82.45%**						
Kappa	**0.78%**						

Accuracy Assessment for 2015

	Mangrove	Other Vegetation	Waterbody	Settlement	Bareground	Classification Overall	Producers Accuracy Precision
Mangrove	61	7	2	0	0	70	**87.14%**
Other Vegetation	2	41	0	2	0	45	**91.11%**
Waterbody	6	0	39	1	0	46	**84.78%**
Settlement	0	4	3	76	7	90	**84.44%**
Bareground	0	3	2	19	28	51	**54.90%**
Truth Overall	69	54	46	98	35	302	
User Accuracy (Recall)	**88.41%**	**75.93%**	**84.78%**	**77.55**	**80%**		
Overall Accuracy(OA)	**81.13%**						
Kappa	**0.76**						

2. Transition Matrix

Transition matrix from 1991 - 2000

	Mangrove	Other Vegetation	Waterbody	Settlement	Bareground
Mangrove	0.43	0.3678	0.1338	0.0414	0.0269
Other Vegetation	0.1775	0.665	0.0443	0.1058	0.0074
Waterbody	0.123	0.168	0.601	0.0369	0.0711
Settlement	0.0722	0.4572	0.0082	0.4447	0.0178
Bareground	0.03	0.1175	0.0463	0.4386	0.3676

Transition matrix from 2000 -2015

	Mangrove	Other Vegetation	Waterbody	Settlement	Bareground
Mangrove	0.6969	0.2643	0.0329	0.0036	0.0023
Other Vegetation	0.0917	0.8283	0.0085	0.0668	0.0047
Waterbody	0.216	0	0.7587	0.004	0.0213
Settlement	0	0.2167	0.0002	0.728	0.0551
Bareground	0.0003	0.044	0.1702	0.2248	0.5606

3. Pictures from Field